Ionospheric Irregularities Across African Sector: Observation Perspective

J. Olwendo[1] & P. J. Cilliers[2]

[1]Pwani University, Department of Physics, Box 195-80108, Kilifi-Kenya.
[2]South African National Space Agency, Hermanus, South Africa.

African CAPACITY BUILDING WORKSHOP IN SPACEWEATHER EFFECT ON GNSS, 3RD-14TH October, 2022. ICTP-Italy

Outline

❖Motivation: Why should we be concerned about Ionospheric Irregularities?

❖Where do irregularities come from? Low latitude/equatorial Electrodynamics

❖How to observe variable PRE using TEC measurements?

❖The post-midnight PRE? What causes it?

❖Measurement Techniques for Irregularities in the Ionosphere

❖Observations of Ionospheric Irregularities across the Africa sector

❖Understanding the Morphology of Irregularities using a dense grid of GNSS receivers on the ground

❖Other forms of Irregularities related to post-sunset TEC perturbations -TIDs

❖Summary

❖References

Ionization levels from ground observations: Smooth vs. Irregular Ionosphere

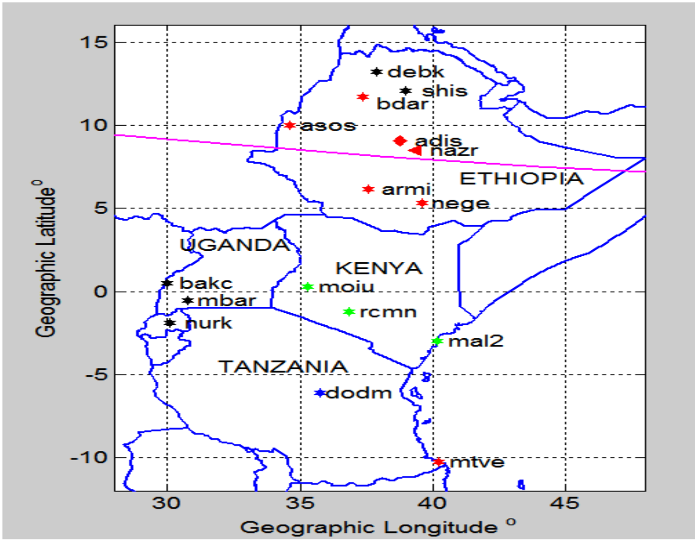

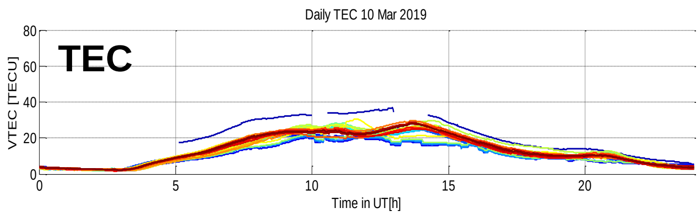

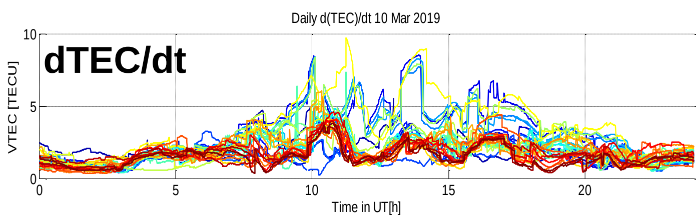

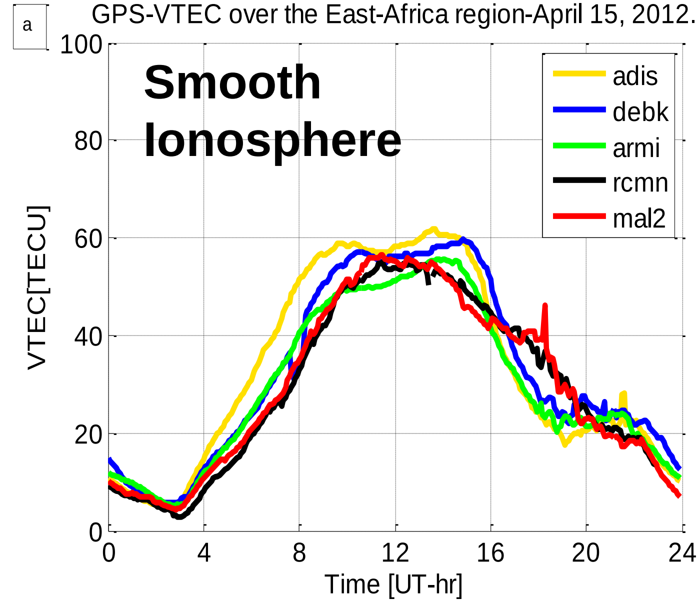

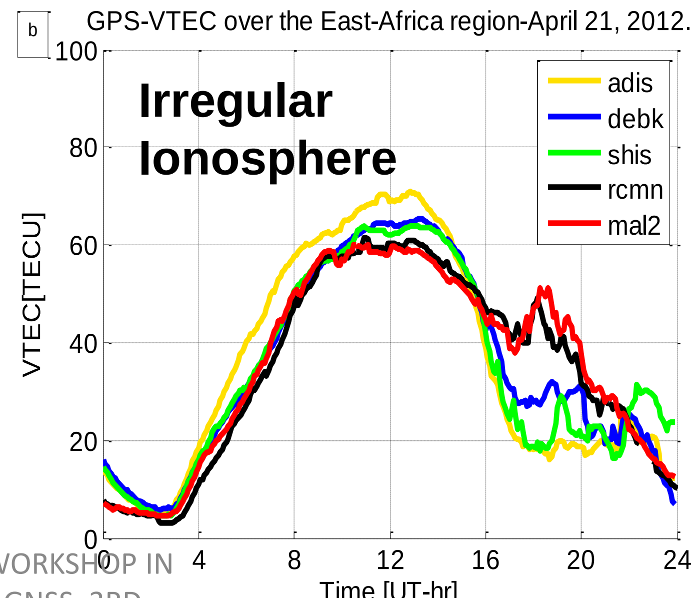

The ionization throughout the day is smooth with VTEC variations arising from change in ionization levels based on solar zenith angle. After sunset VTEC irregularities appear due to EPBs causing fluctuations in ionization density.

Irregularities mainly dominant at night: Africa region observed from space

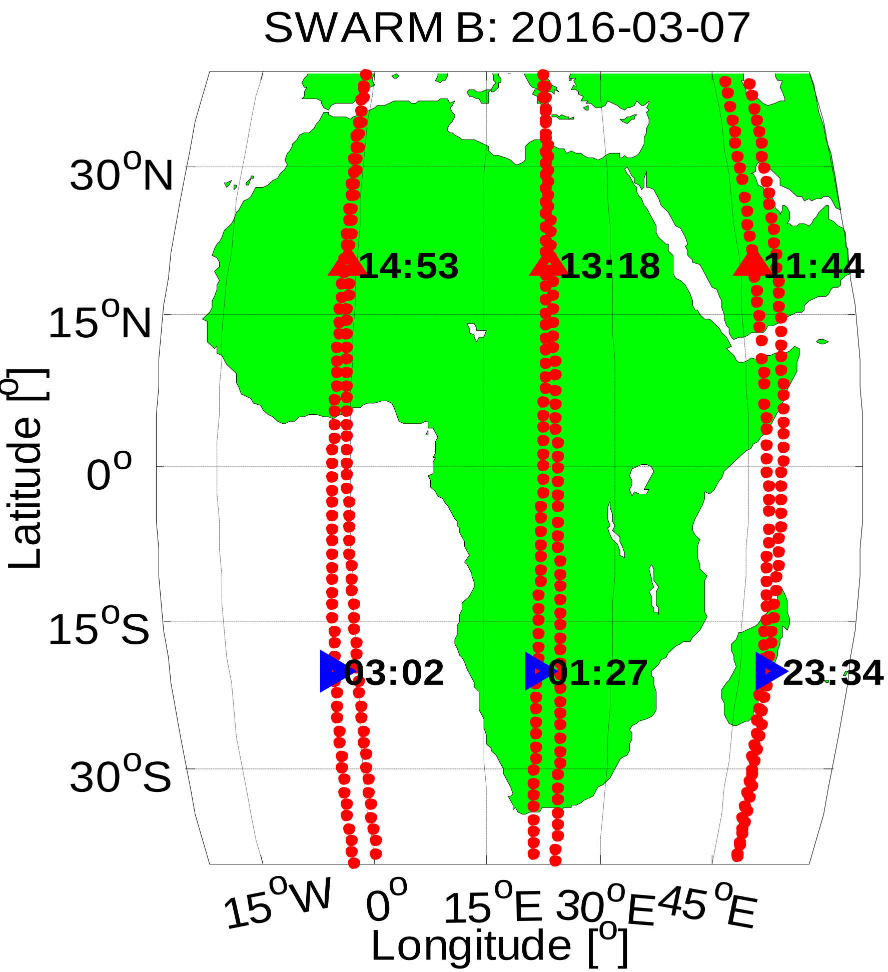

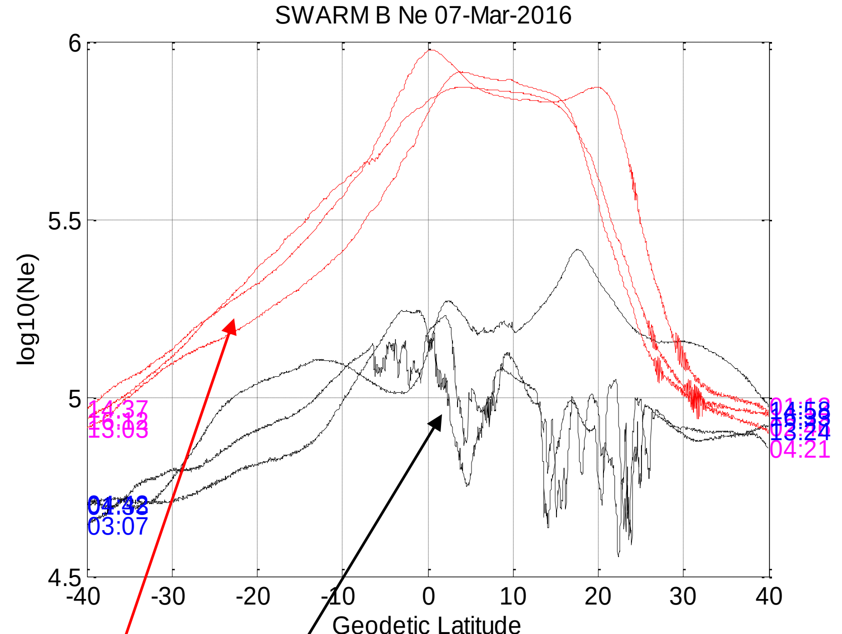

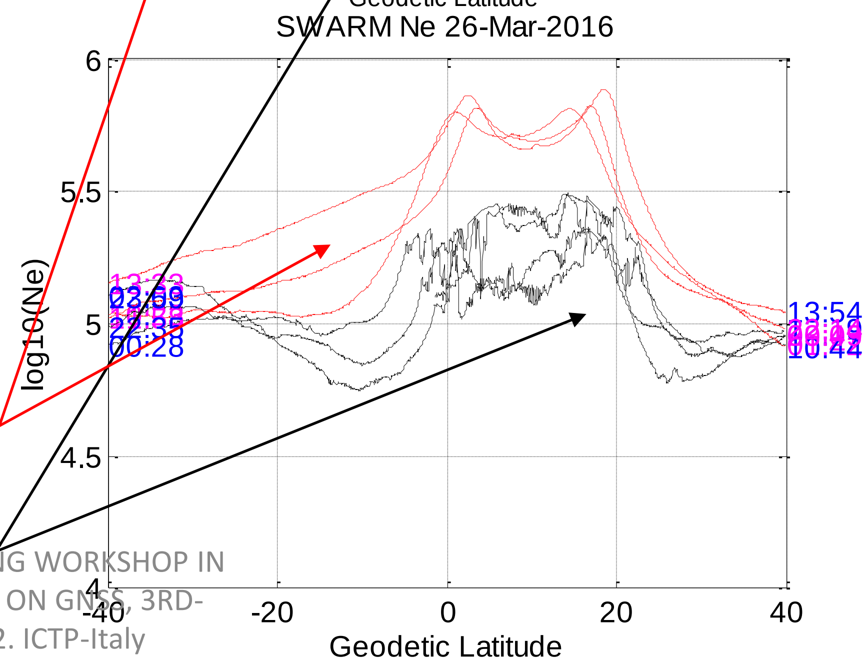

Red lines show day-time is in-situ electron density measurements by the Swarm B satellite.
Black lines show in situ measurements during the post sunset hours.

Why should we be concerned about irregularities?
Motivation 1 : Impact on Technology and Human Activity (Economy)

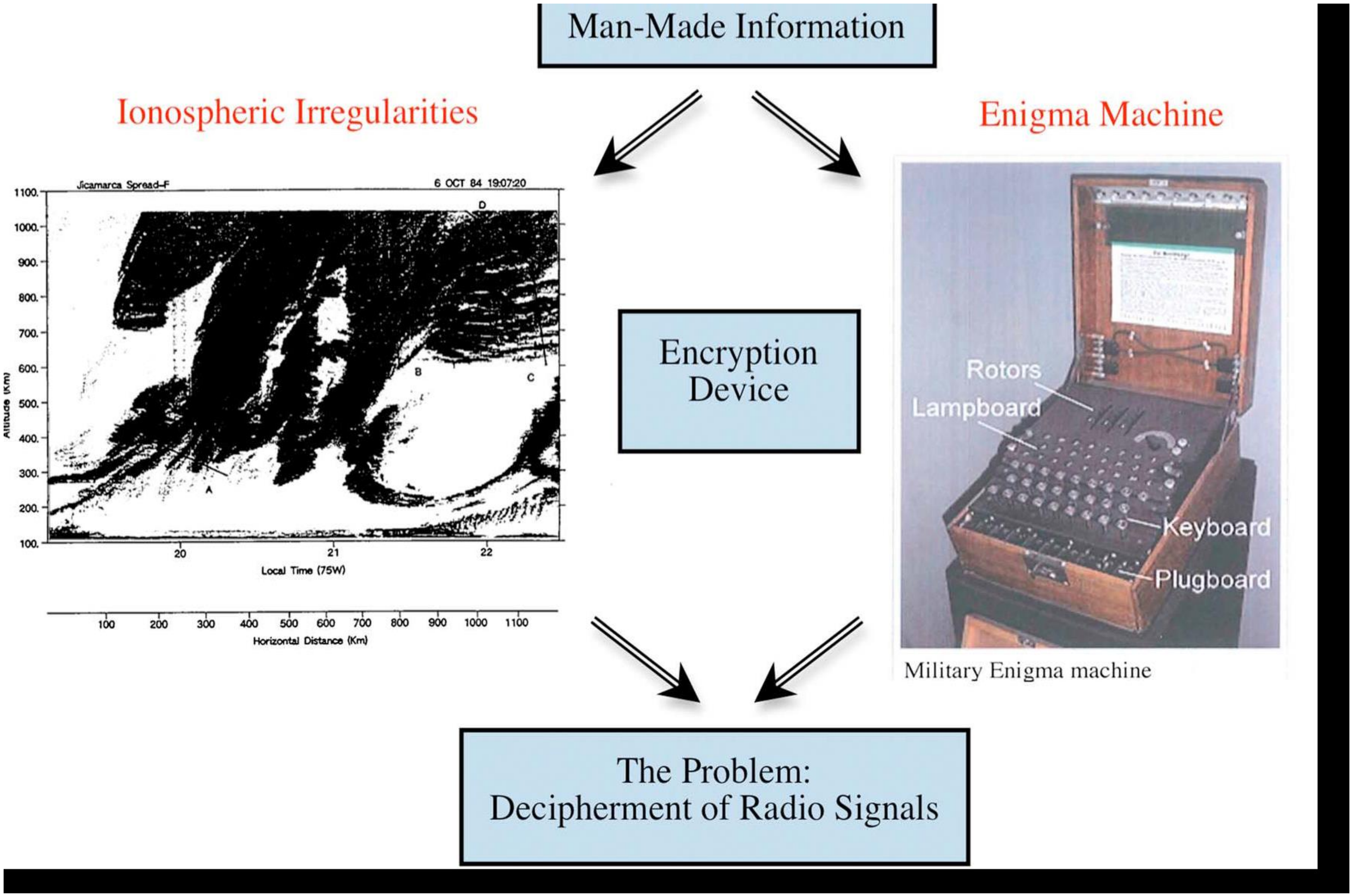

Courtesy: **Jan Sojka SPACE WEATHER, VOL. 11, 134–137, doi:10.1002/swe.20041, 2013**

What happens to GNSS signals in the presence Ionospheric Irregularities? And what can we do about it?

Phase Screen Model

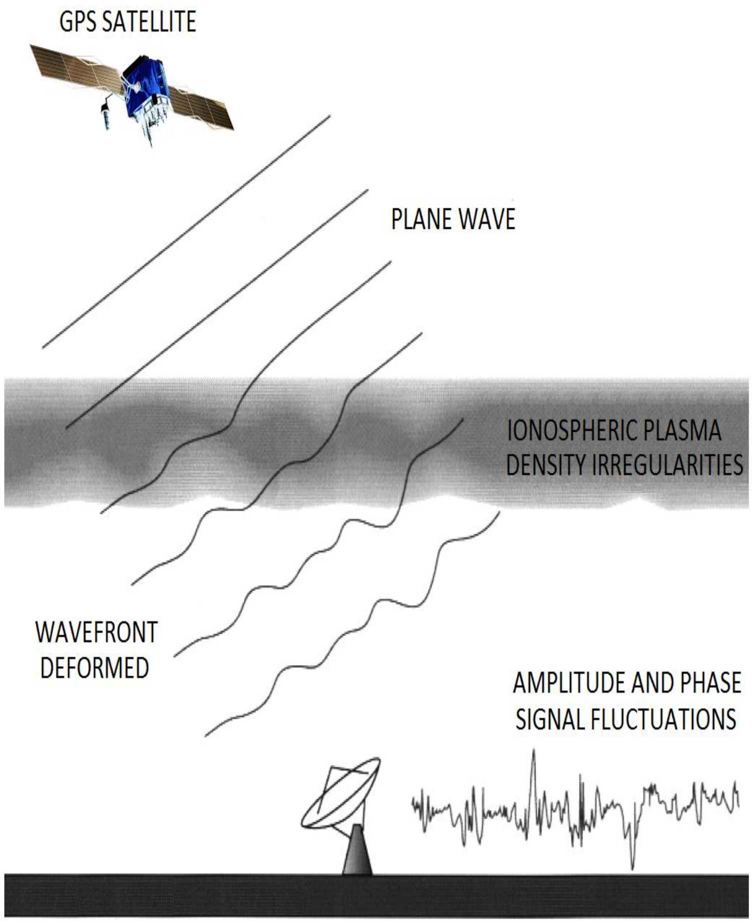

- **At the screen only the phase is modulated**
- **As the wave propagates beyond the screen, diffraction causes variations in the amplitude**
- **Larger scale-size irregularities dominate as the wave propagates further and further from the screen (z increases**

GNSS as a stand-alone research infrastructure: Motivation 2

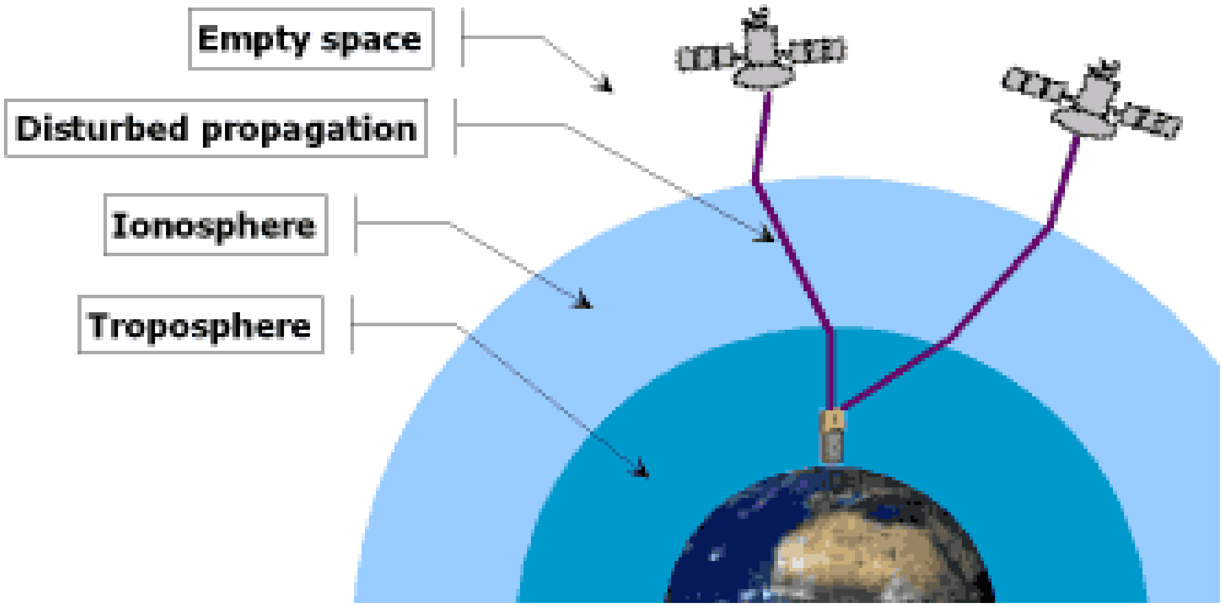

- Seismic monitoring & prediction
- Volcano monitoring
- Climate change
- Gravity fields
- Atmospheric science:
    - atmospheric water vapor
    - the ionosphere
    - space weather

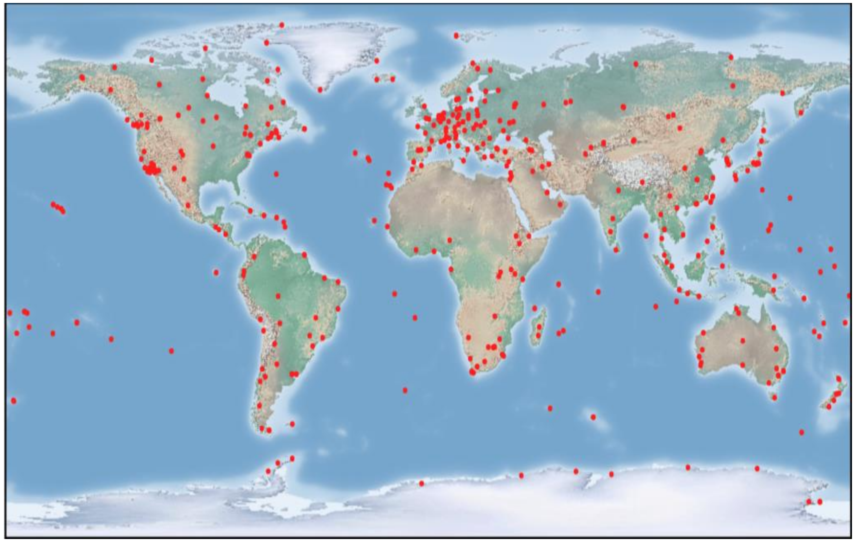

IGS Receivers, Last Updated 2019
Source: https://www.igs.org/station-resources/

Where do irregularities come from in the low latitude Ionosphere?

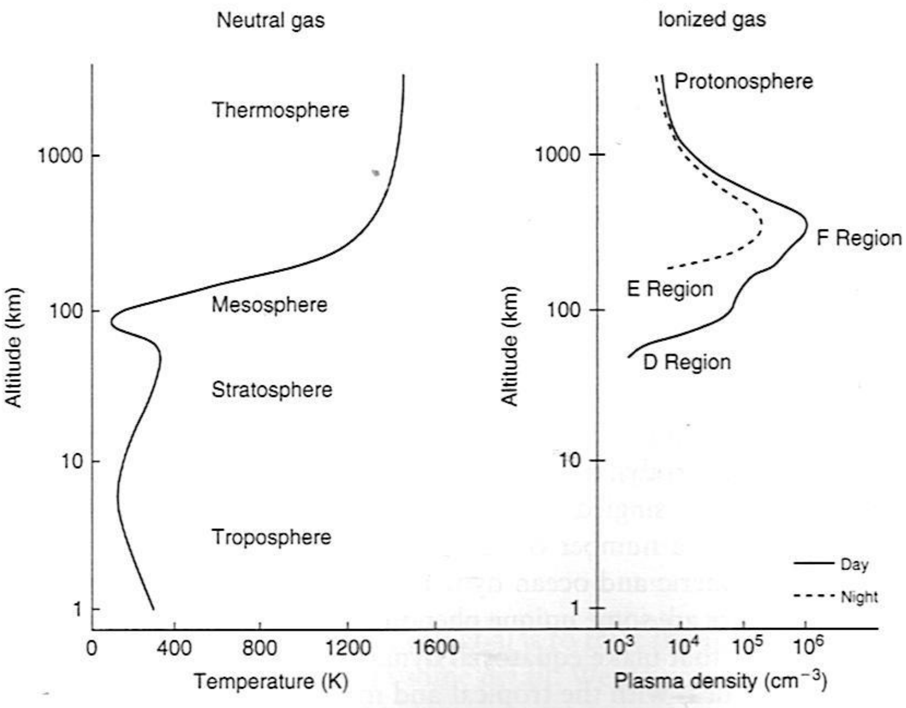

plasma

- charged particles
- $n \approx n_i \approx n_e$

•Motion influenced by: gravity (g), pressure (p), Magnetic field (B) and Electric field (E)

ν_{jn} : Collisions with neutrals

Momentum Equation: Steady state

Gravity — Electric Field — Collision Freq with neutrals — Neutral wind velocity

$$0 = -k_B T_j \vec{\nabla} n + nM_j \vec{g} + ne(\vec{E} + \vec{V}_j \times \vec{B}) - nM_j \nu_{jn} (\vec{V}_j - \vec{U})$$

Pressure — Magnetic Field

Ionospheric dynamics at post-sunset hours

Towards dusk the enhanced zonal E-field is established to keep divergenc J = 0 from a sharp east-west (day-night) conductivity (density) gradient Zonal E leads to pre-reversal enhancement (PRE) in the eastward electric field.

The F- layer thus rises as the ionosphere co-rotates into darkness. The ionization in the lower part rapidly decays and a steep vertical density gradient develops leading to a classical Rayleigh-Taylor (R-T) instability.

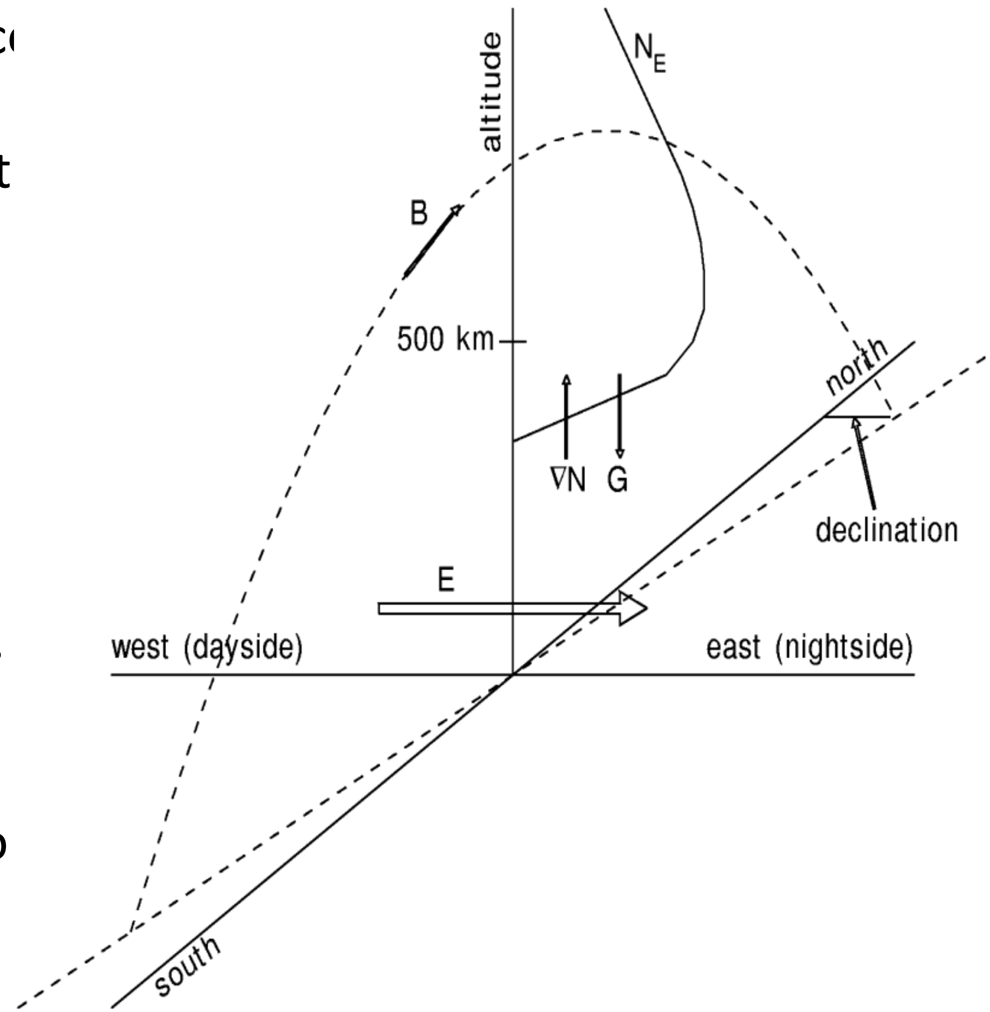

Schunk and Nagy, 2009, Figure 11.29

What is the mechanism behind PRE?

❖ PRE can be explained in terms of the F-region dynamo and its coupling to E-region: based on the field line integrated electric fields models. The PRE mechanisms are:

a) Hall current divergence mechanism- Farley et al., (1986)
b) High cowling conductivity –Haerendel and Eccles, (1992/
c) Curl-free mechanism –Eccles, 1998

❖ PRE is primarily due to the curl free nature of the electric fields.

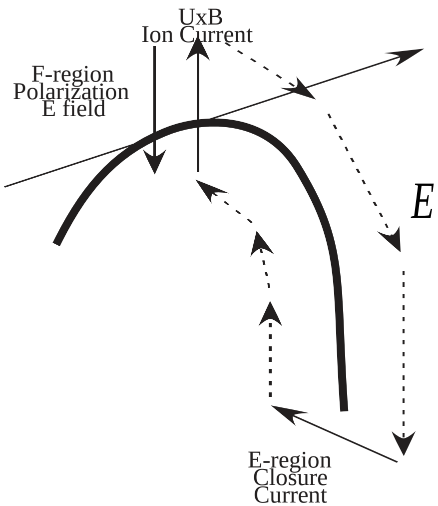

$$E = -\frac{\sum_P^F}{\sum_E^P + \sum_F^P} U_F \times B$$

Current loop driven by zonal winds in the F region.

Source: R.A. Heelis, JASTP, 66 (2004) 825– 838

- F-region wind is eastward thus associated field is downward in the equatorial region.
- Downward electric field is not uniform in the zonal direction but has a strong eastward gradient due to rapid decay of E conductivity and eastward wind acceleration of F region.
- The curl of electric field must be zero, this requirement leads to an eastward electric field that corresponds to the large upward vertical drift of the PRE.

Post Sunset Ionospheric Electrodynamics

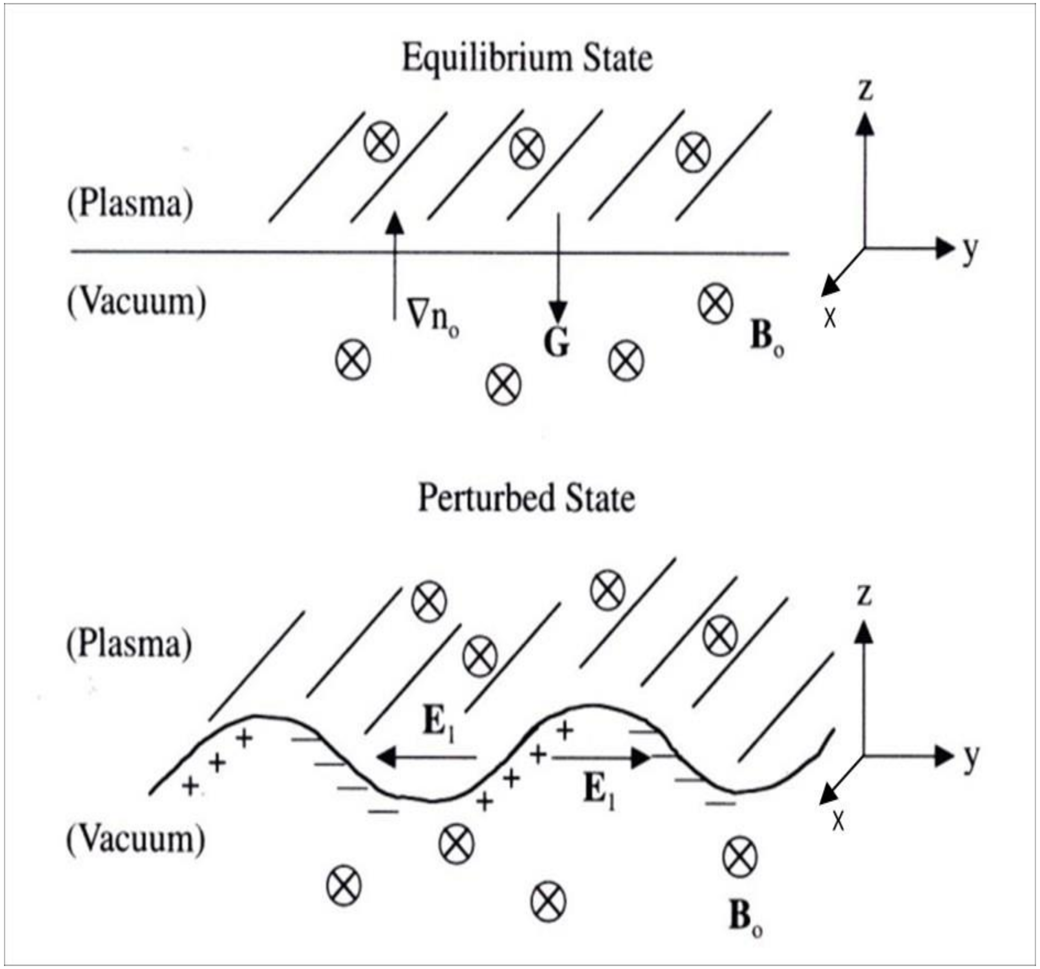

Plasma instability: RT scenario

1. Sharp vertically upward gradient of plasma density.

2. Horizontal magnetic field lines

3. Currents driven by background electric fields

4. Gravity

All are mutually perpendicular

[Schunk nd Nagy, 2009, Figure 11.30

Bottom side unstable due to perturbation: density gradient against gravity.

Observations of turbulent post sunset low latitude ionosphere

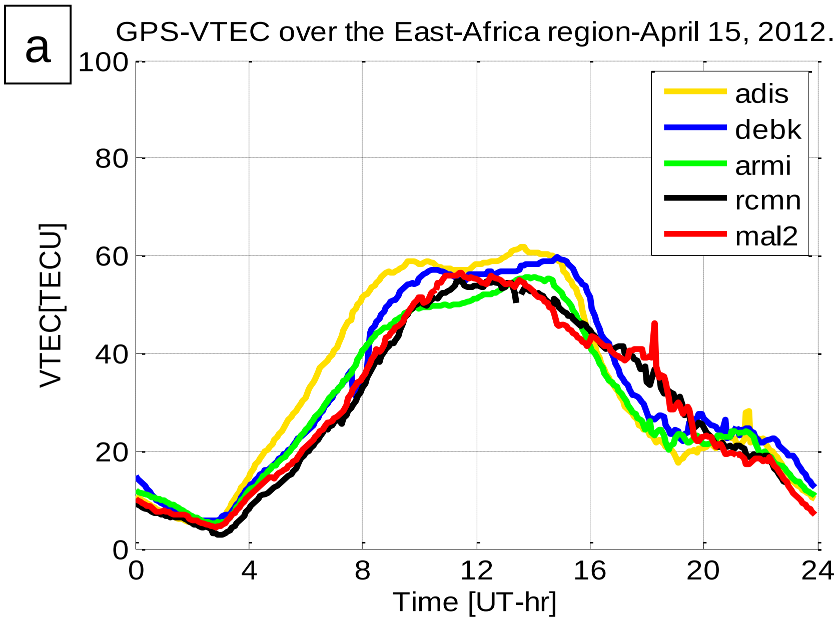

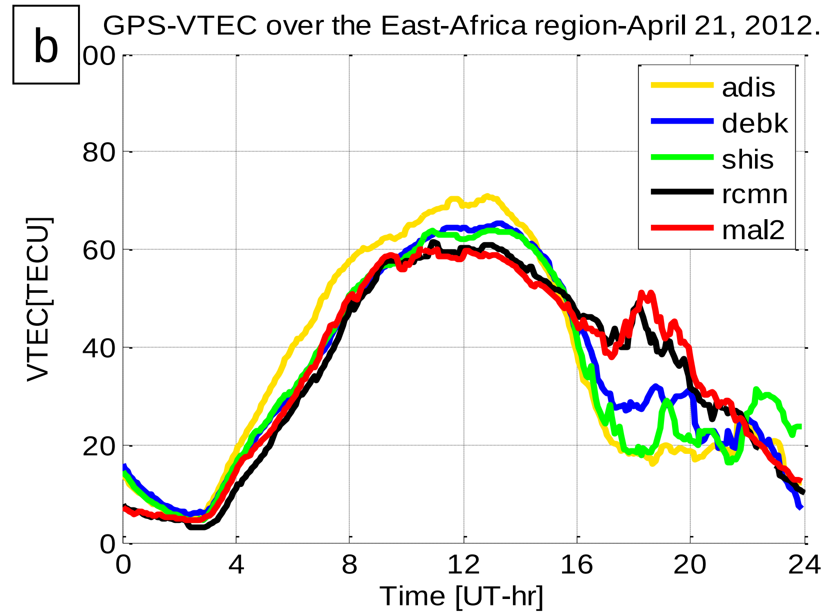

The **black** arrow shows an intense EEJ at sunset-local-PRE.
This could be the cause of intense post-sunset TEC enhancement on 21-April (Fig b)

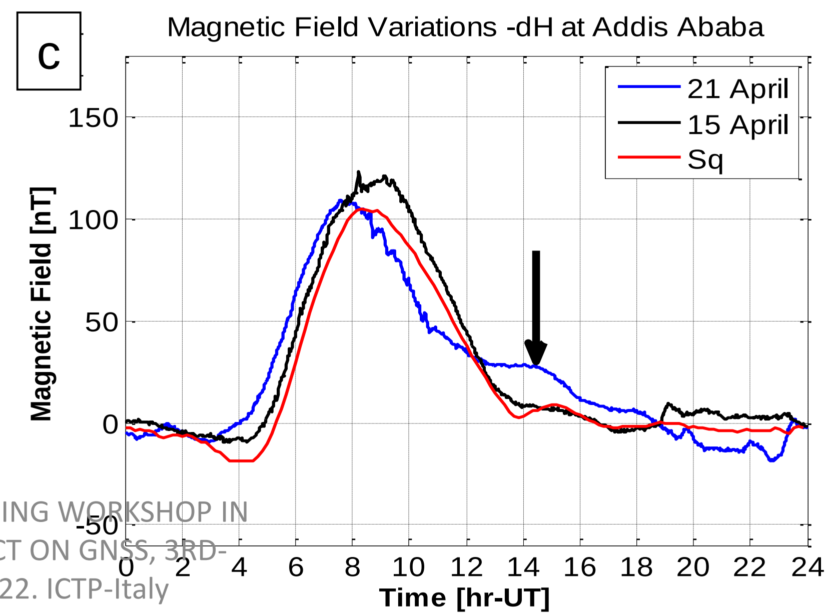

PRE= Prereversal Enhancement of East-ward electric field

How variable is the Post-sunset enhancement?

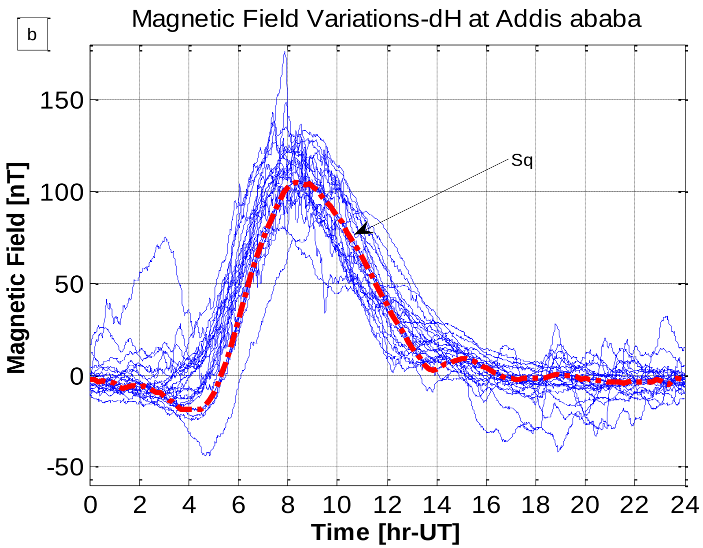

Post sunset enhancement is highly variable and depends on the magnitude of the PRE.

PRE cause plasma to be uplifted at the dip equator. It then moves to the regions North and South of the dip equator and fluctuations in PRE leads to variability in TEC

Question? In the absence of PRE, do we still have the post-sunset TEC enhancement?

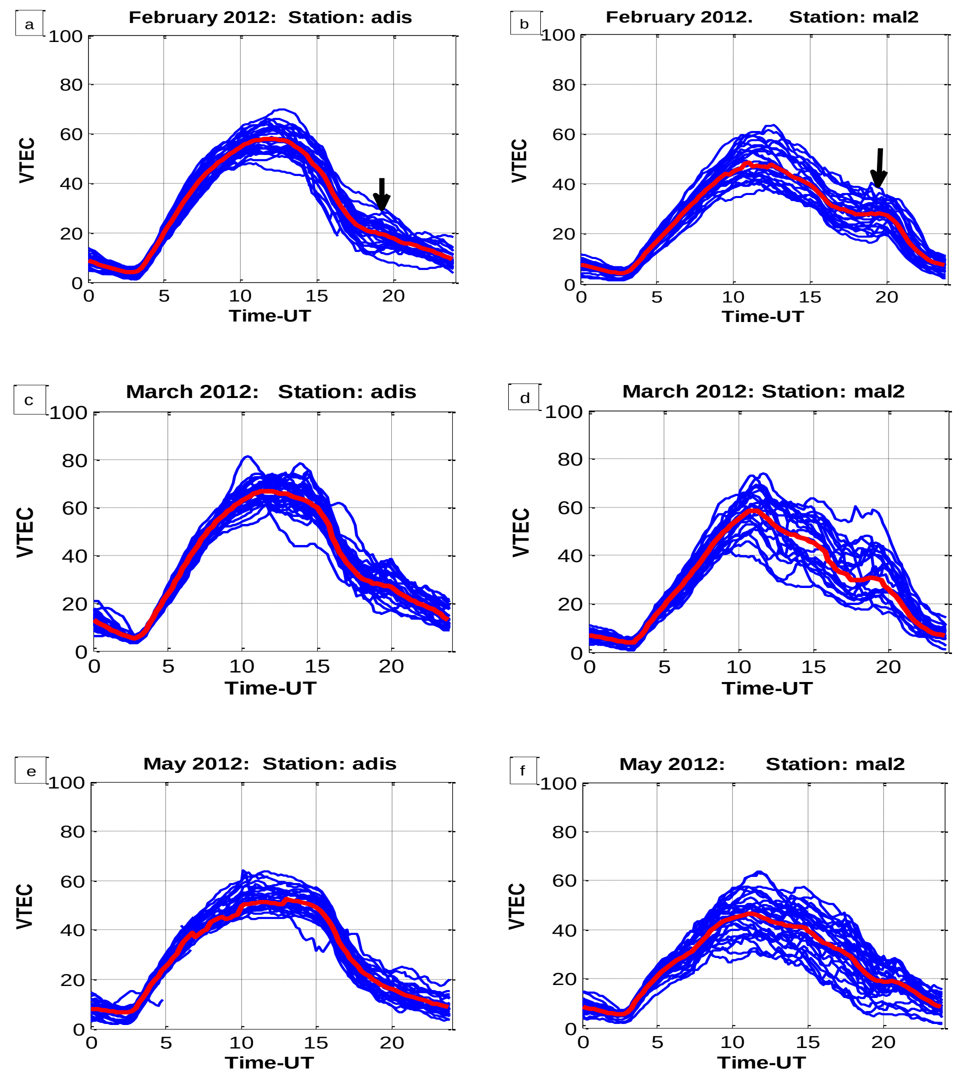

Depletions occur at dip equator at sunset and enhancements occur North and South of the dip equator.

Irregularity monitoring across Africa using IGS network:

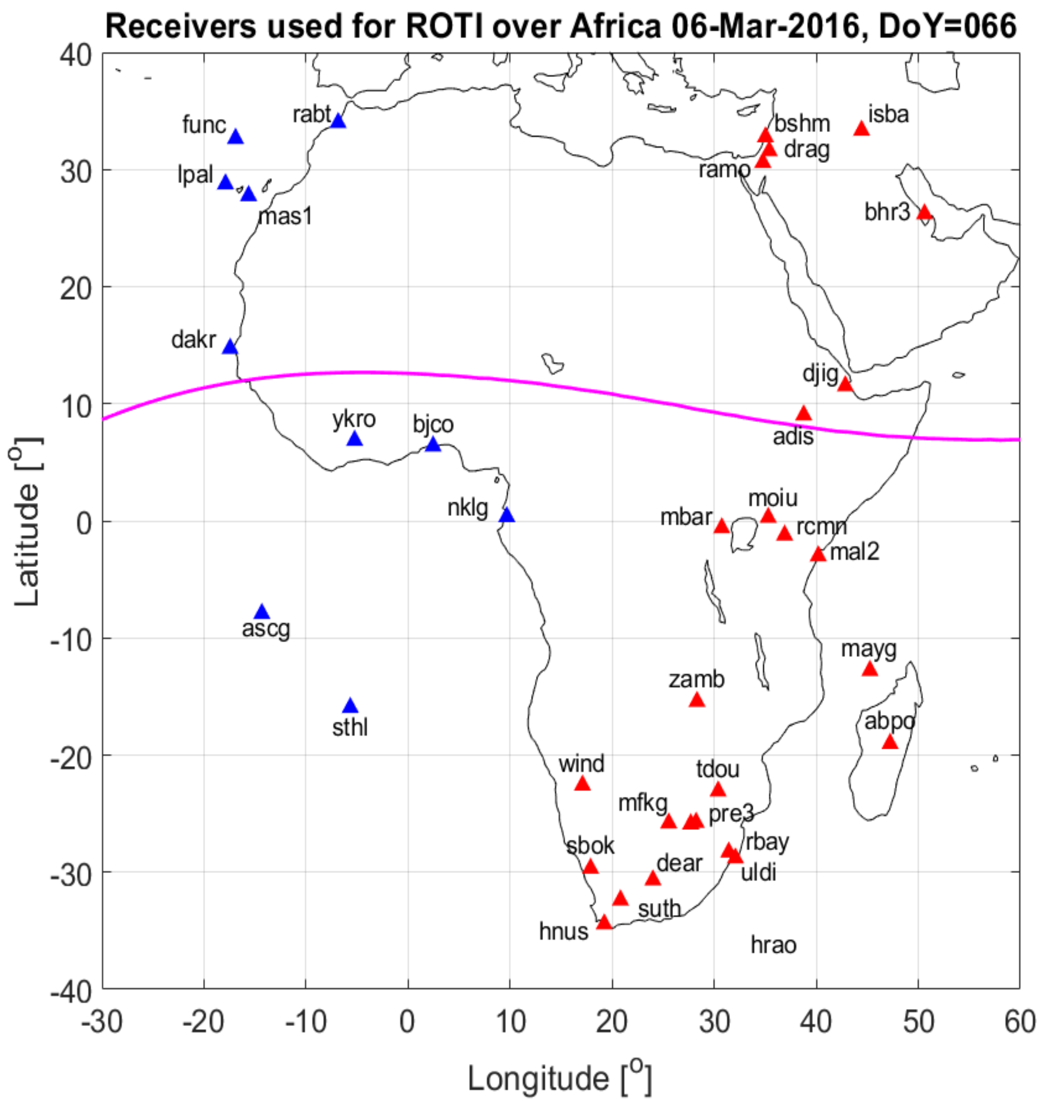

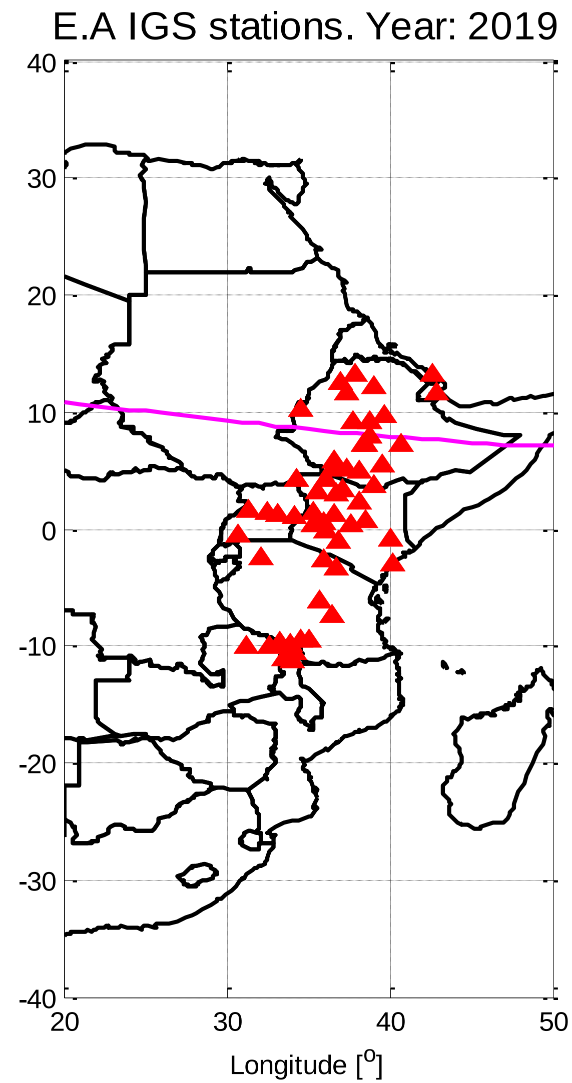

Post-sunset TEC enhancement associated with Irregularities: East Africa sector

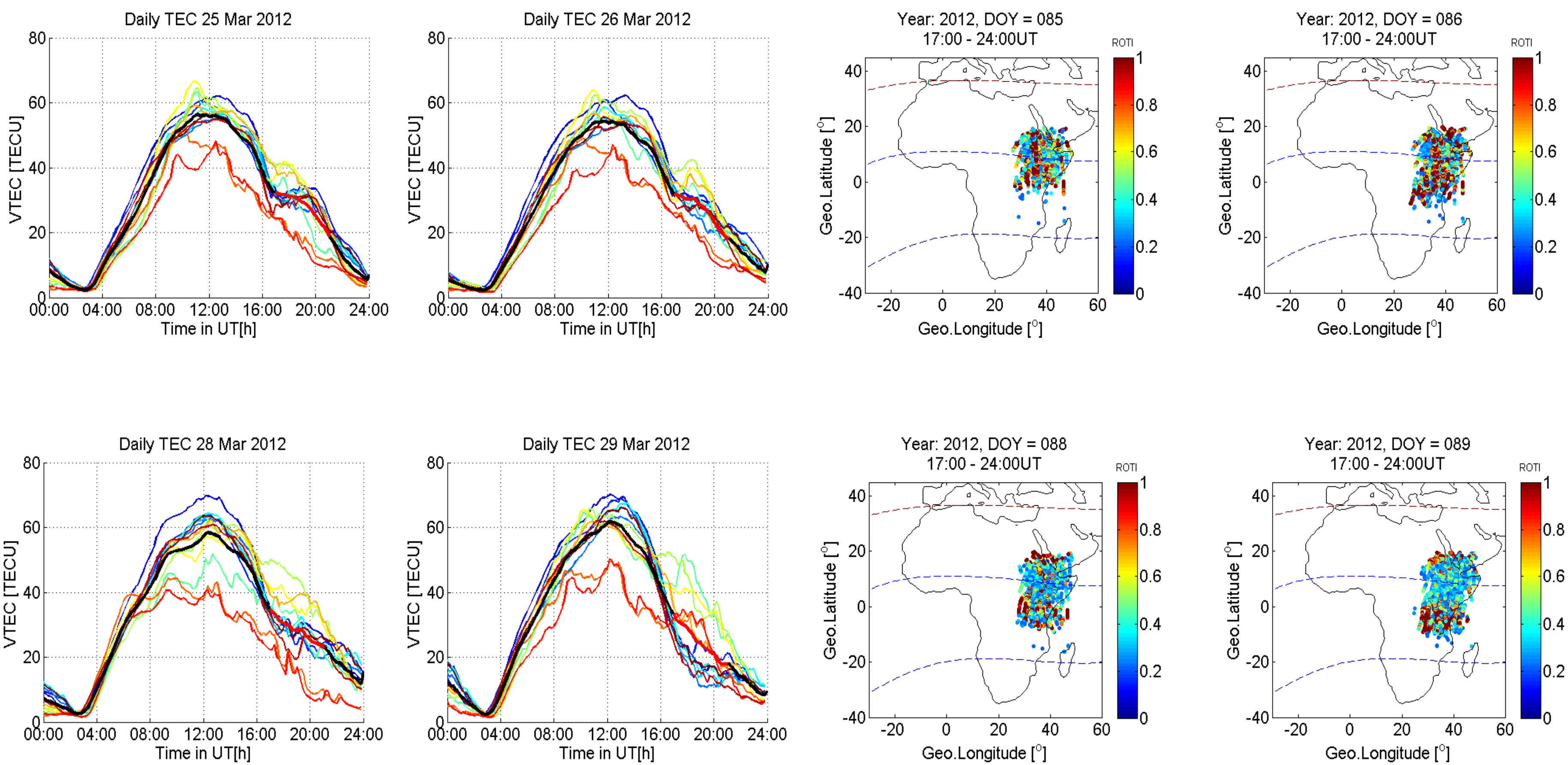

TEC enhancement remains a precursor of a fully developed PRE via the plasma vertical drift to the F region where ionization dominates.

Post Sunset TEC enhancement associated with No Irregularities

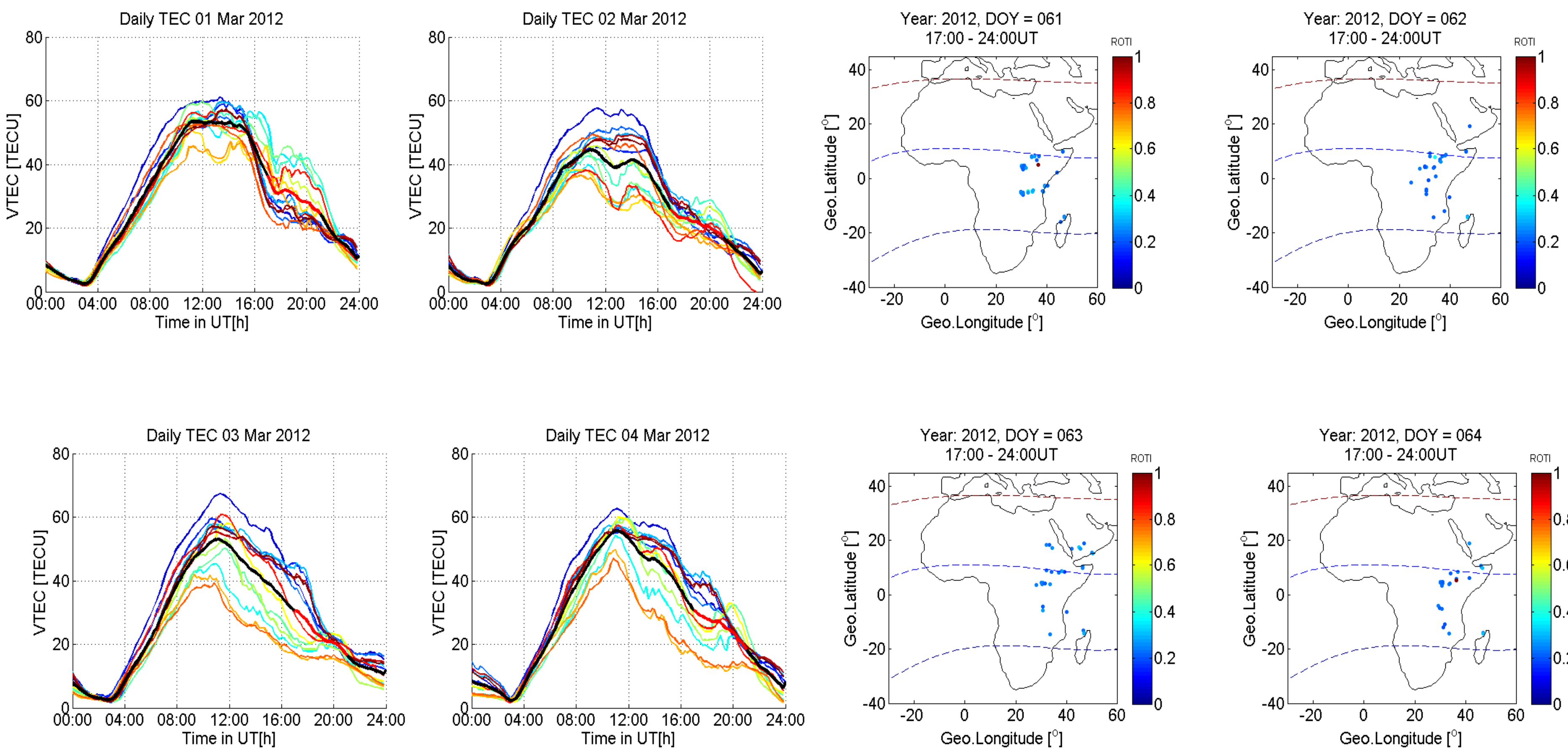

No irregularity days: No TEC enhancements after post sunset hours

Post Midnight PRE starting after 21:00 UT

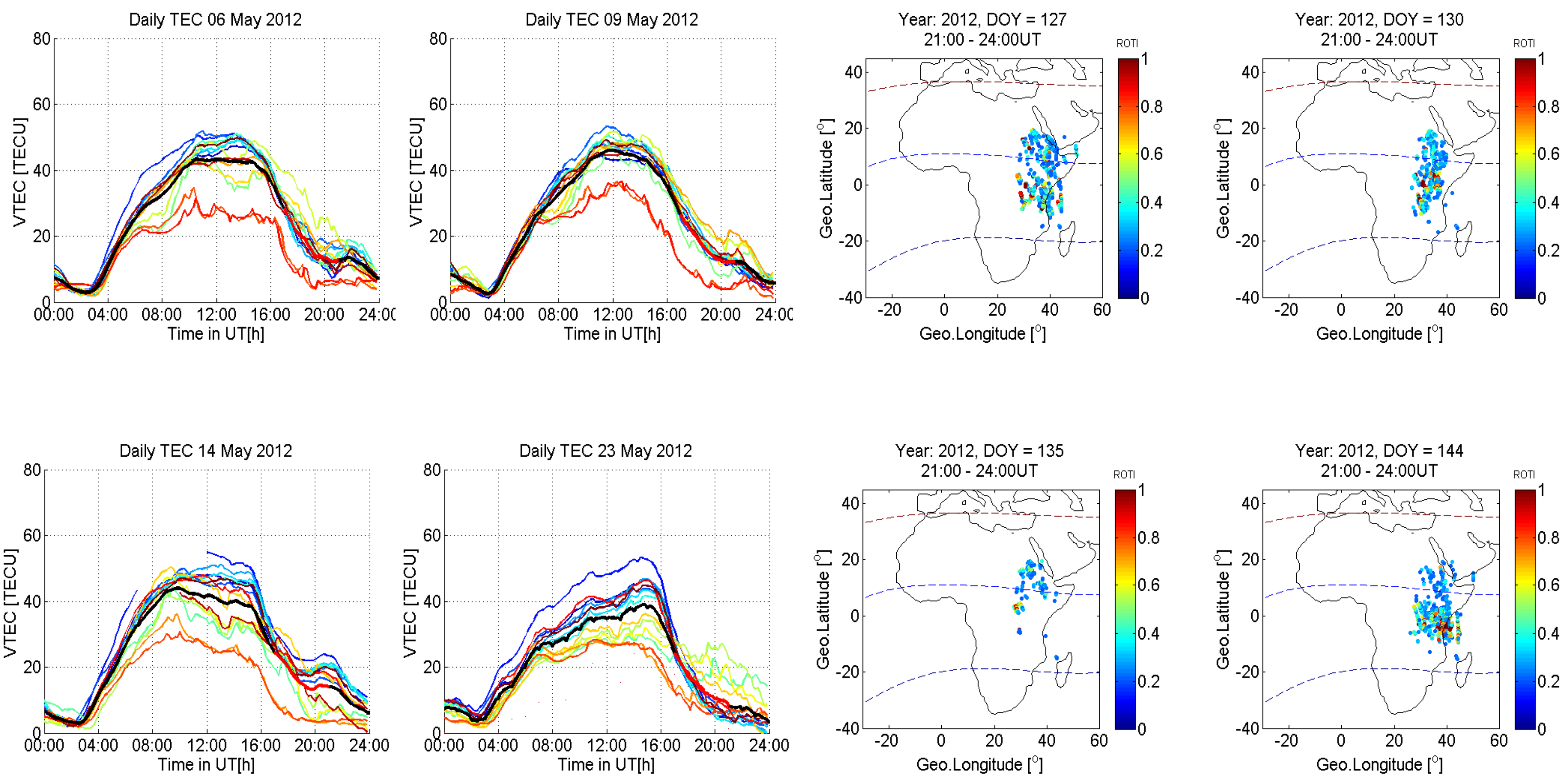

While the PRE varies with solar condition, season, and longitude it o exhibits night-to-night variability that currently defies prediction.

Is the post midnight pre also linked enhanced eastward electric fields? Where are they from?

What Triggers the formation of ionospheric irregularities?

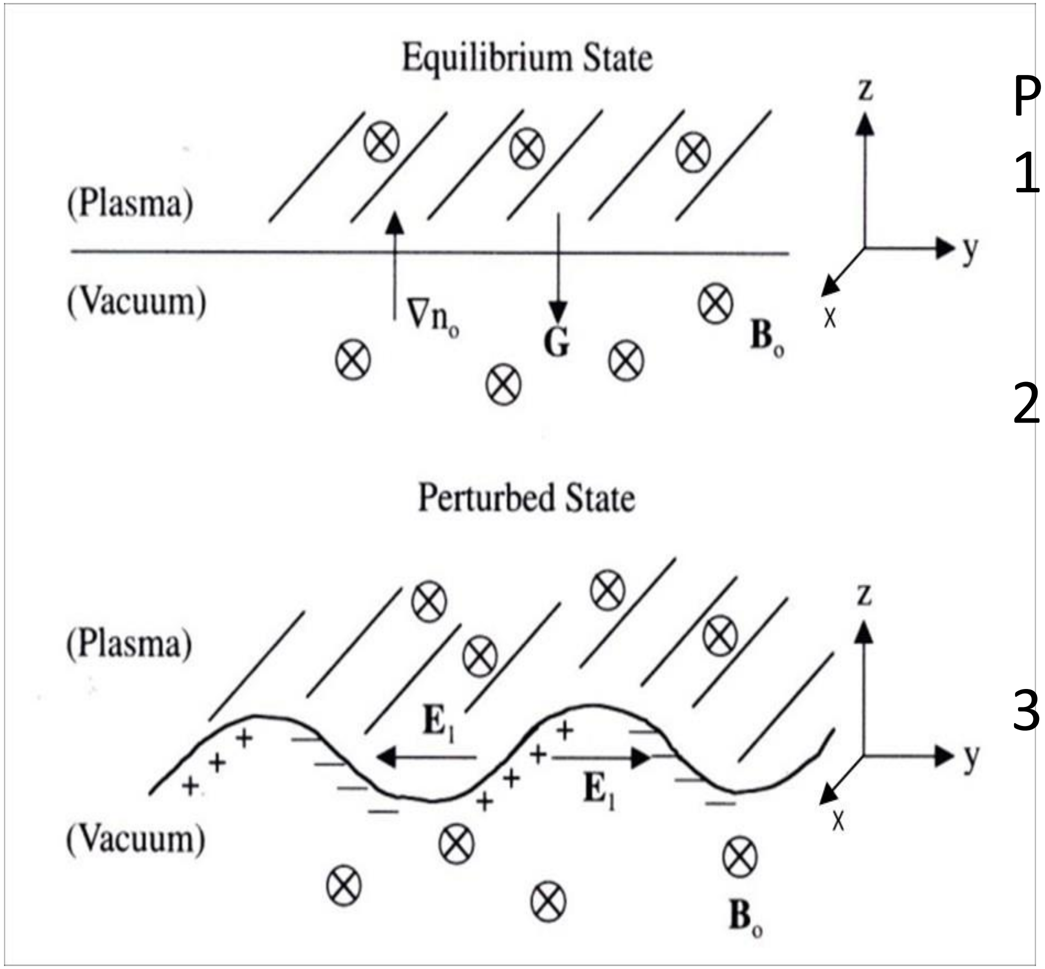

Plasma instability: RT scenario

1. Sharp vertically upward gradient of plasma density.

2. Pressure driven current does not create any perturbation electric fields

3. Pressure driven current flow parallel to the modulated density pattern and has no divergence.

[Schunk nd Nagy, 2009, Figure 11.30

Linear Theory of Rayleigh-Taylor Instability

Steady-state momentum equation

$$0 = -\underline{k_B T_j \vec{\nabla} n} + \boxed{nM_j \vec{g}} + ne(\overset{0}{\vec{E}} + \boxed{\vec{V}_j \times \vec{B}}) - nM_j \overset{0}{\nu}_{jn}(\vec{V}_j - \vec{U})$$

J is proportional to density $\quad J = ne(V_i)_\perp = nM_i \vec{g} \times \frac{\vec{B}}{B^2}$

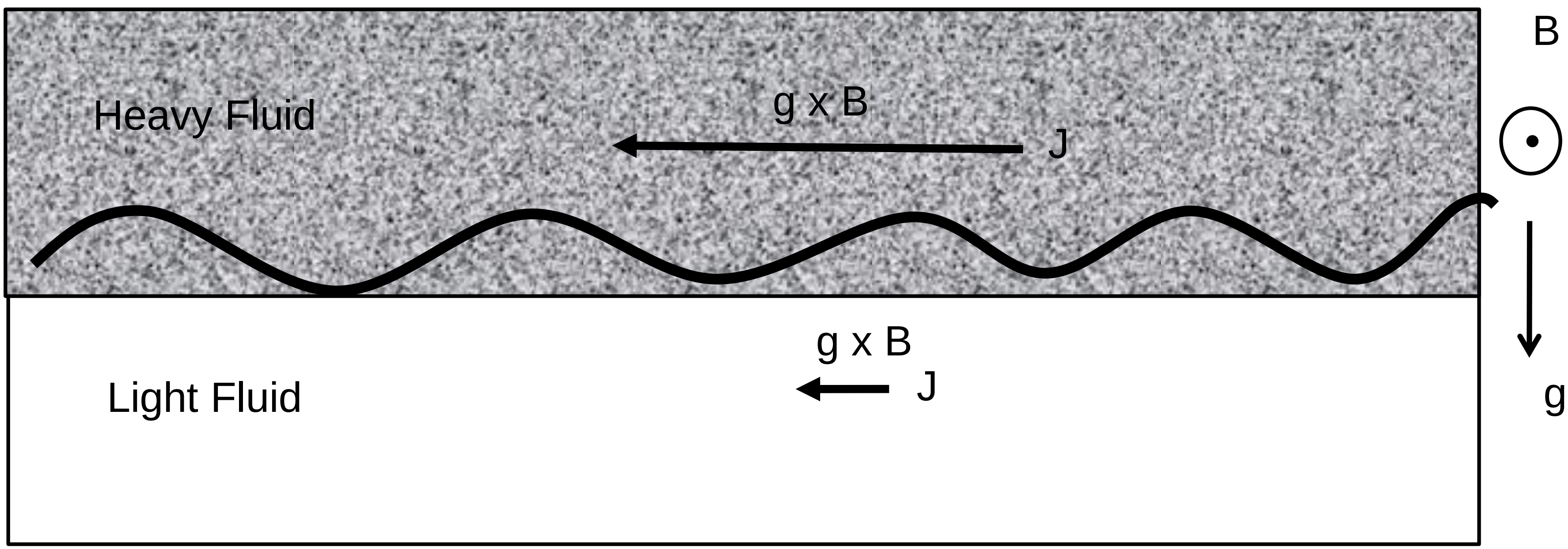

Linear Theory of Rayleigh-Taylor Instability

Steady-state momentum equation

$$0 = -k_B T_j \vec{\nabla} n + \boxed{nM_j \vec{g}} + ne(\overset{0}{\vec{E}} + \boxed{\vec{V}_j \times \vec{B}}) - nM_j \overset{0}{\nu_{jn}} (\vec{V}_j - \vec{U})$$

J is proportional to density

$$J = ne(V_i)_\perp = nM_i \vec{g} \times \frac{\vec{B}}{B^2}$$

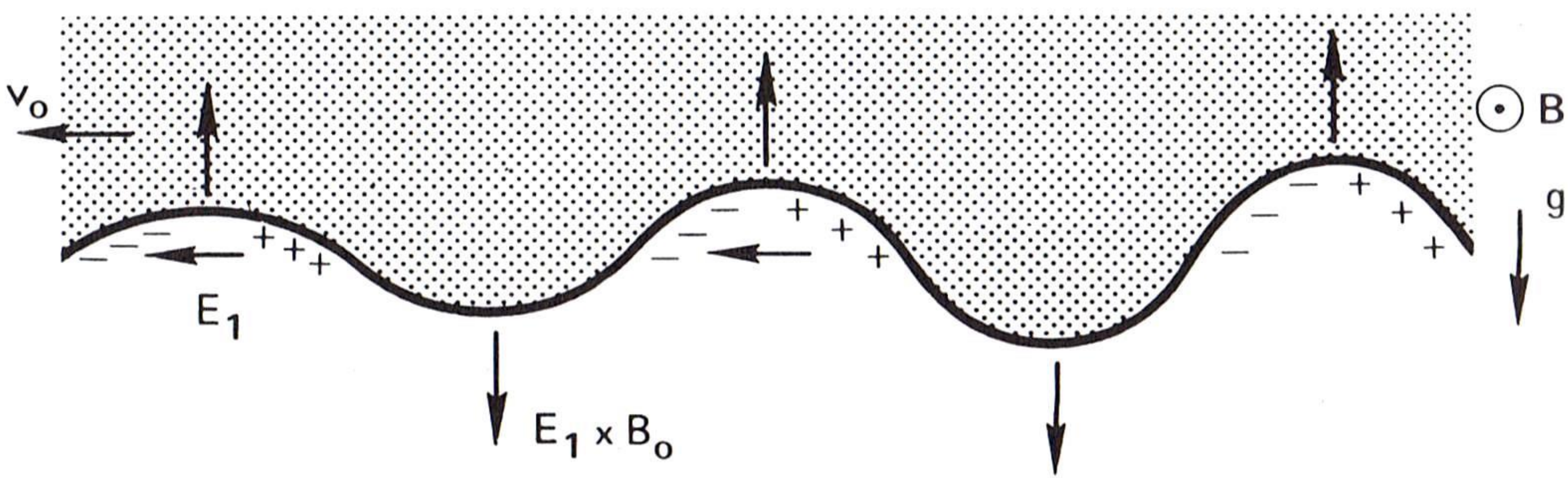

Image from F. F. Chen, Plasma Physics textbook

Post Sunset Ionospheric Electrodynamics

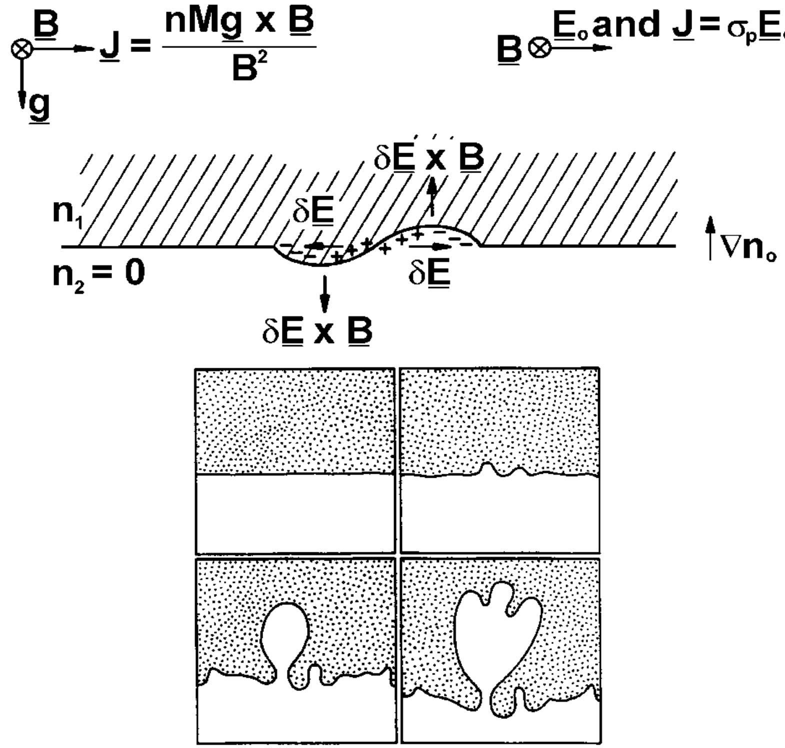

[Schunk and Nagy, 2009, Figure 11.30

An exponential growth of instability

$$A = A_0 e^{\gamma t}$$

$$\gamma \approx \frac{\sum_F}{\sum_F + \sum_E}\left[\frac{\boldsymbol{E}\times\boldsymbol{B}}{B^2} + U_n + \frac{g}{\nu^{eff}}\right]\frac{1}{N}\frac{\partial N}{\partial h}$$

Non-linear Rayleigh-Taylor Instability

Credit: Prof Ron Caton of AFRL – PBMOD

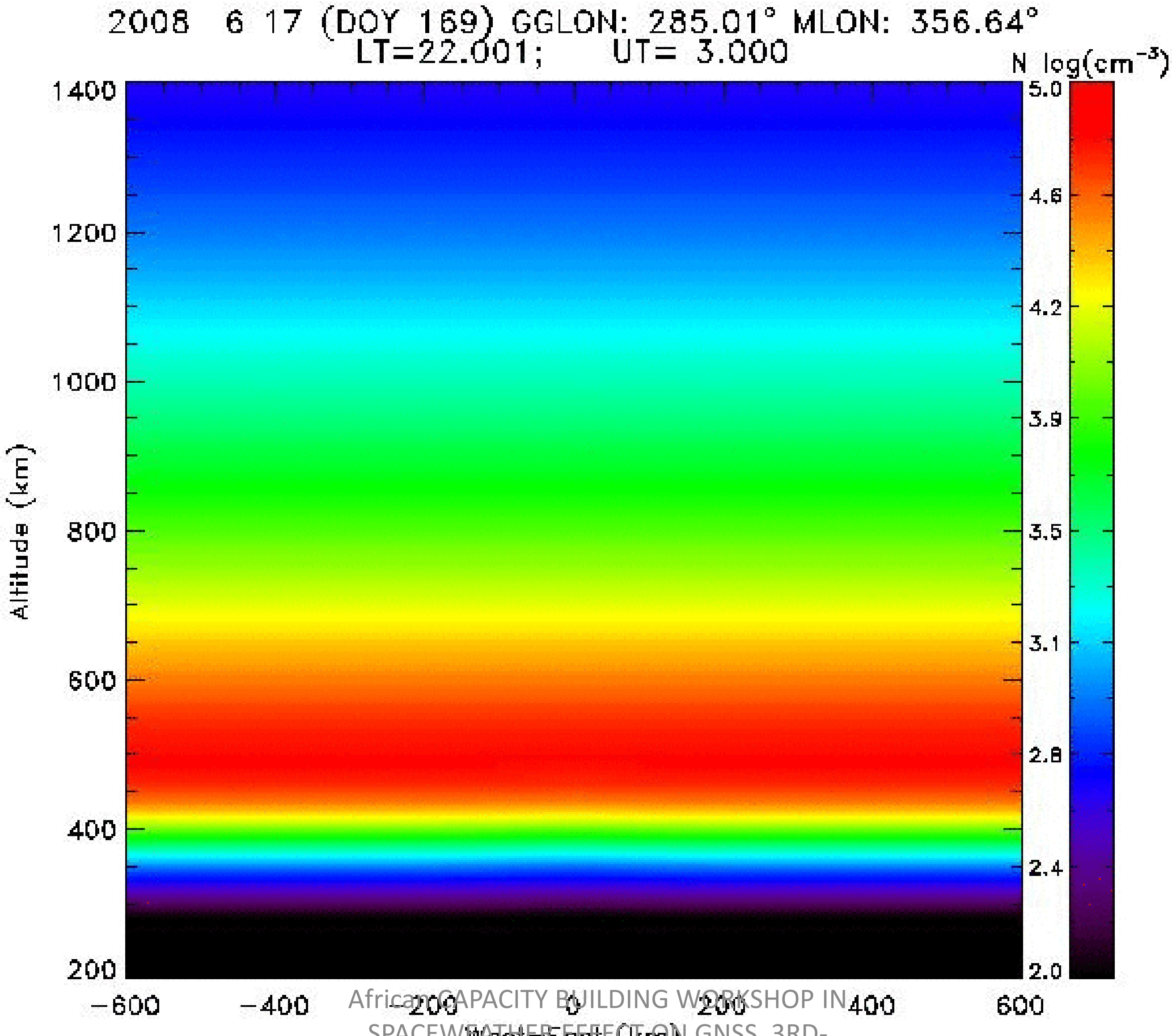

Conditions favourable for irregularity formation into multi-scale sizes

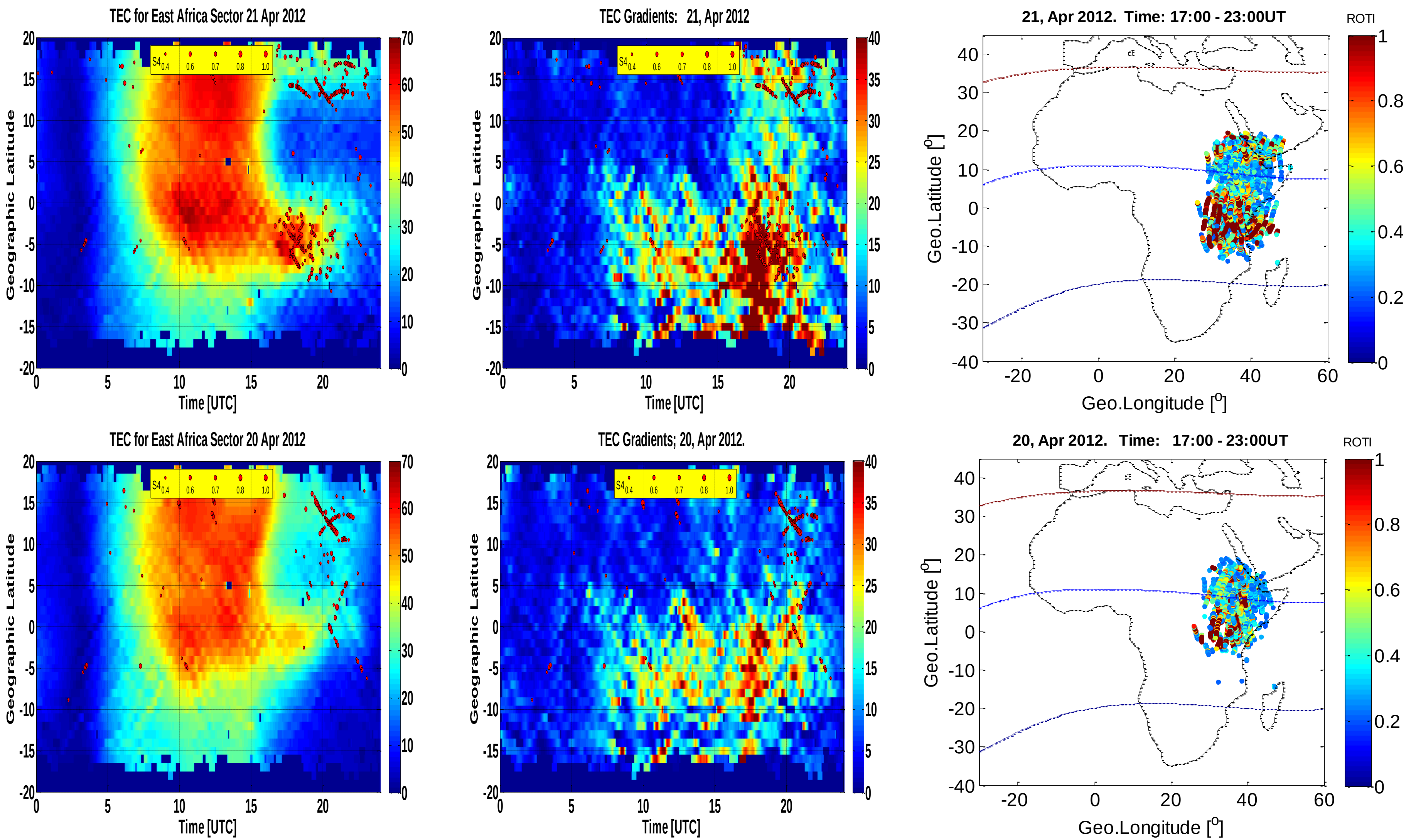

GIM for 26 Mar 2016, 18:00 UT to 21:00 UT

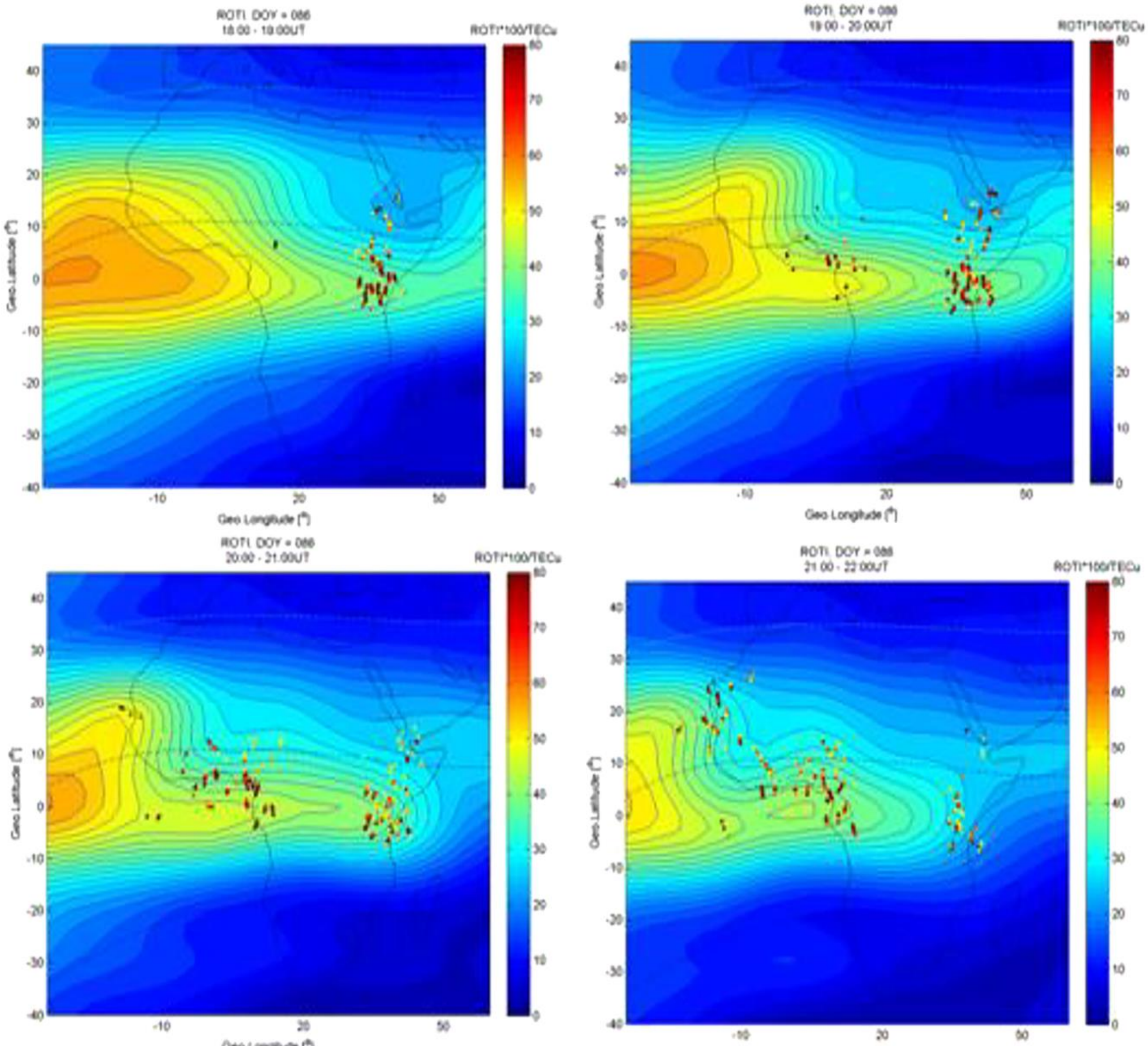

Olwendo et al 2019
Radio Science, *54*.
https://doi.org/
10.1029/2018RS006734

Question to participants:

1. Why don’t we have ionospheric irregularities forming during daytime?

2. Why do the ionospheric irregularities develop near the dip equator/magnetic equator?

Daytime irregularity formation

We can have man induced instability at the bottom of the ionosphere that can cause depletions during daytime similar to the post sunset depletions

1. Daytime F-region irregularity triggered by rocket-induced ionospheric hole over low latitude:

Li et al. Progress in Earth and Planetary Science (2018) 5:11
https://doi.org/10.1186/s40645-018-0172-y

2. Large ionospheric TEC depletion induced by the 2016 North Korea rocket

Byung-Kyu Choi, Hyosub Kil, Advances in Space Research 59 (2017) 532–541

Why do the ionospheric irregularities/bubbles develop only near the dip equator/magnetic equator?

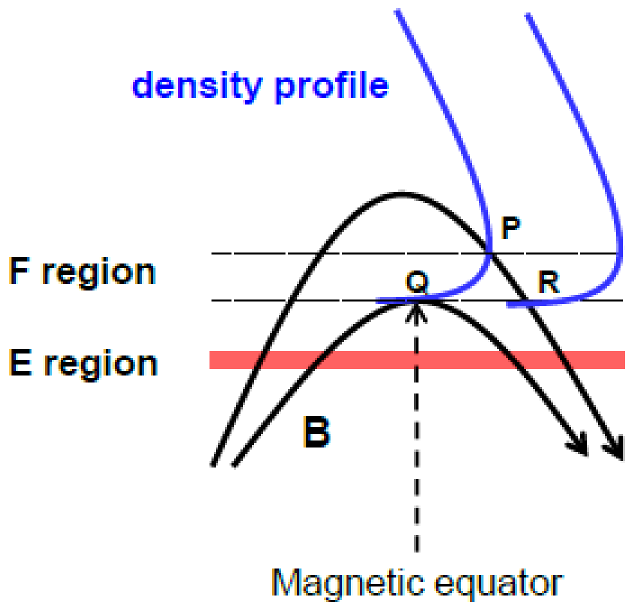

Schematic illustration of the difference of the ionospheric condition at, and off, the magnetic equator

Source: Kil , (2015) J. Astron. Space Sci. 32(1), 13-19.

- At the magnetic equator during the nighttime, Q Region is not connected to higher conductive region, i.e. polarization electric fields in Q can survive longer time.
- Since P and Q are not connected by the same magnetic field lines, electrons from P cannot short out the electric field in Q.
- Off the magnetic equator, R and P can be connected along the same magnetic field lines.
- Because of higher electron density in region P, it can short out polarization electric field at region R.
- For this reason, equatorial ionosphere is most favorable for bubbles formation.

How do we detect the irregularities/plasma depletions ?

- Coherent and incoherent scatter radar.
- In-situ satellite-borne space probe
- Radio occultation and scintillation measurement
- Airglow detectors
- Ionosondes

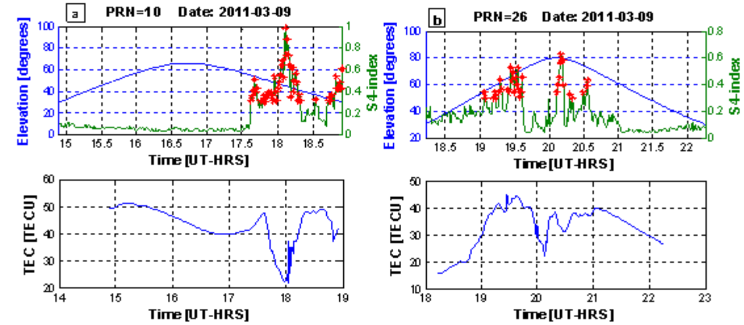

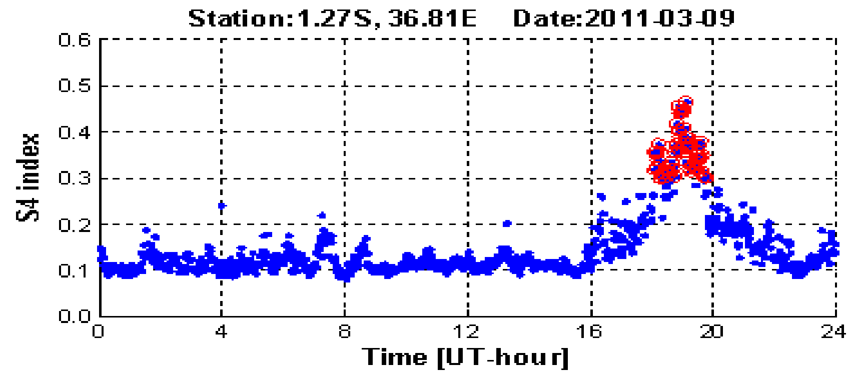

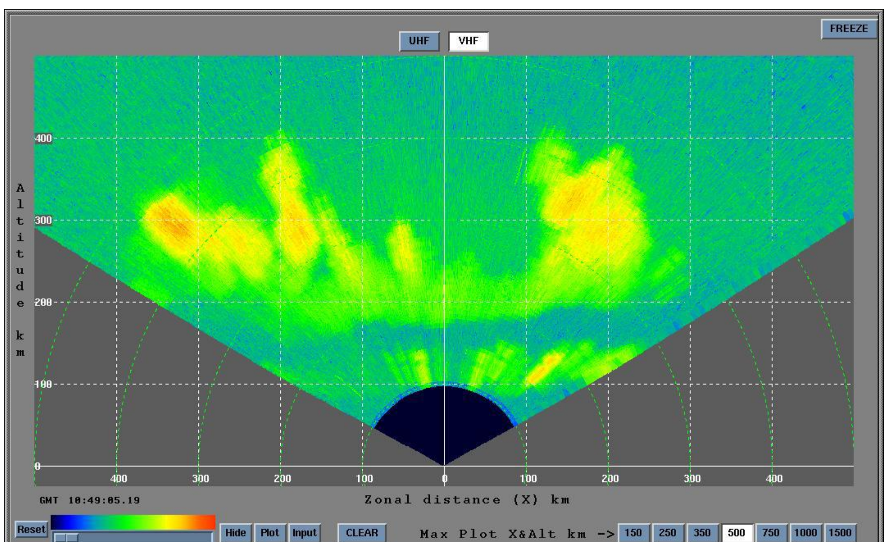

Coherent scatter radar scan
From J. M. Retterer

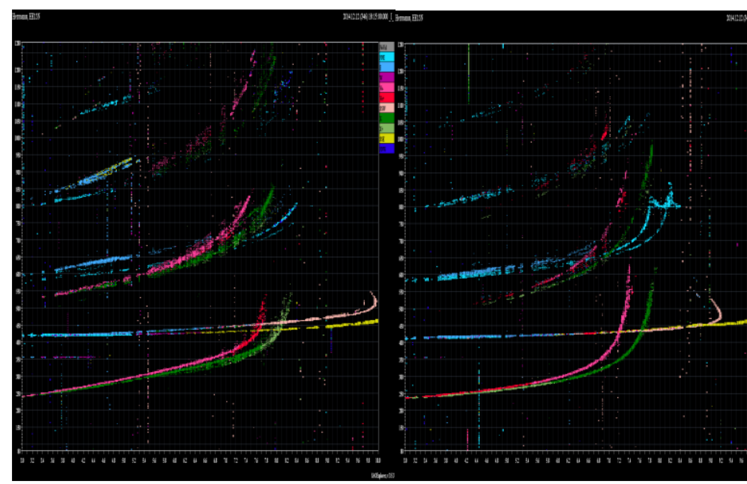

Source: https://sandims.sansa.org.za/

Research Techniques and methodology

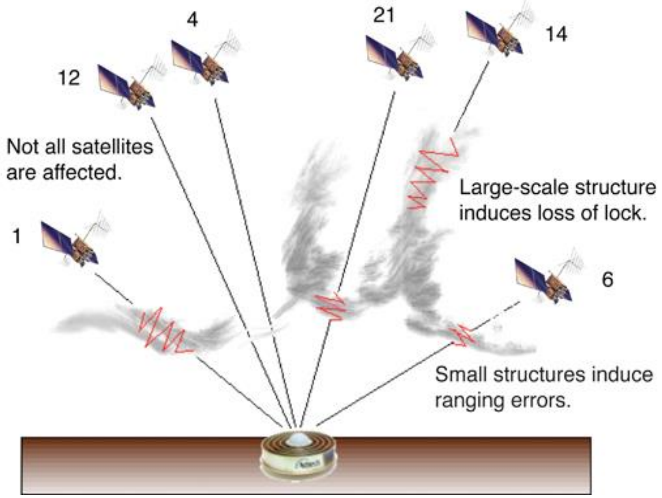

From "Effect of Ionospheric Scintillations on GNSS—A White Paper", SBAS Ionospheric Working Group, November 2010

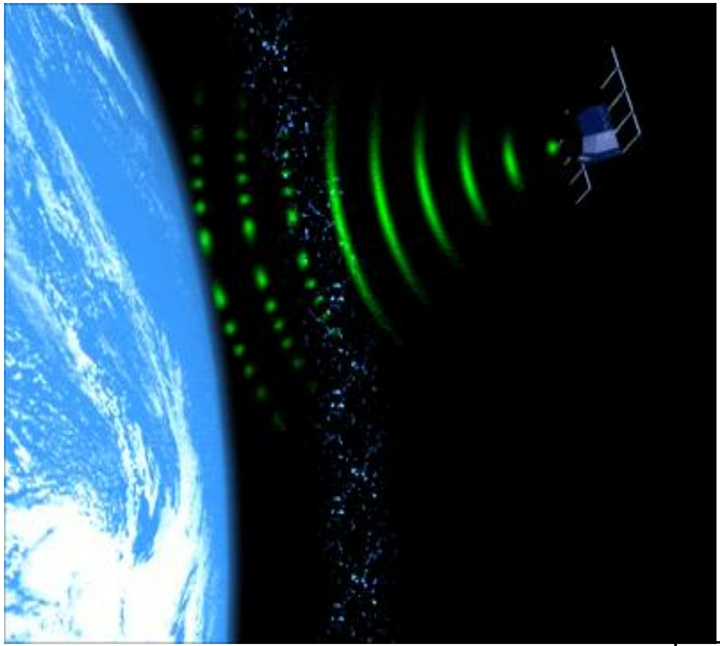

Courtesy: Bath University

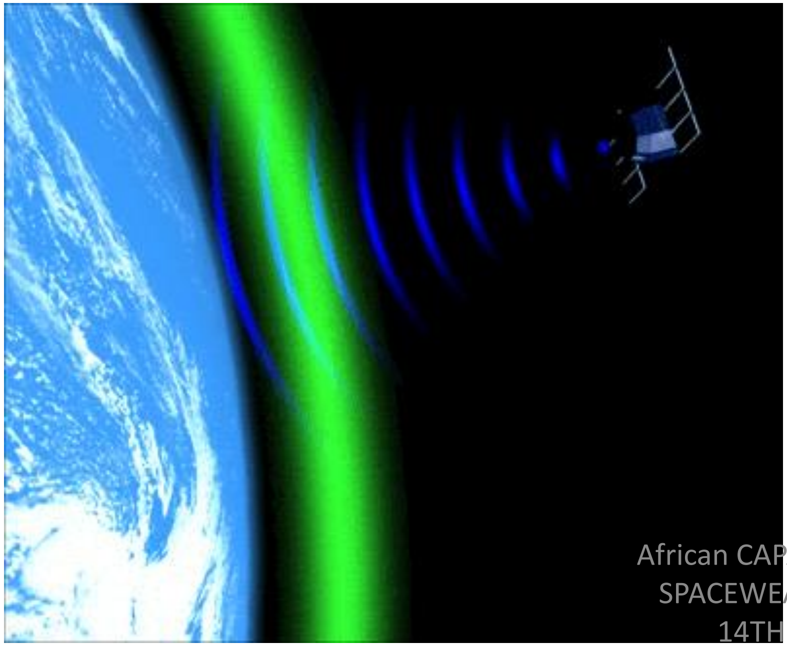

Amplitude Scintillation

$$S_4 = \sqrt{\frac{\langle I^2 \rangle - \langle I \rangle^2}{\langle I \rangle^2}}$$

$$ROT = \frac{TEC_k^i - TEC_{k-1}^i}{t_k - t_{k-1}}$$

$$ROTI = \sqrt{\langle ROT^2 \rangle - \langle ROT \rangle^2}$$

Irregularity activity based on in-situ electron density variations measured by LEO Satellites e.g. Swarm, CHAMP

1. **Irregularity activity:** $\Delta N / N$ **Dao et al., 2011**

Delta N- difference in electron density from the ambient density

N- ambient density: the envelope connecting the total maxima of electron density evaluated at a given time with a spline interpolation

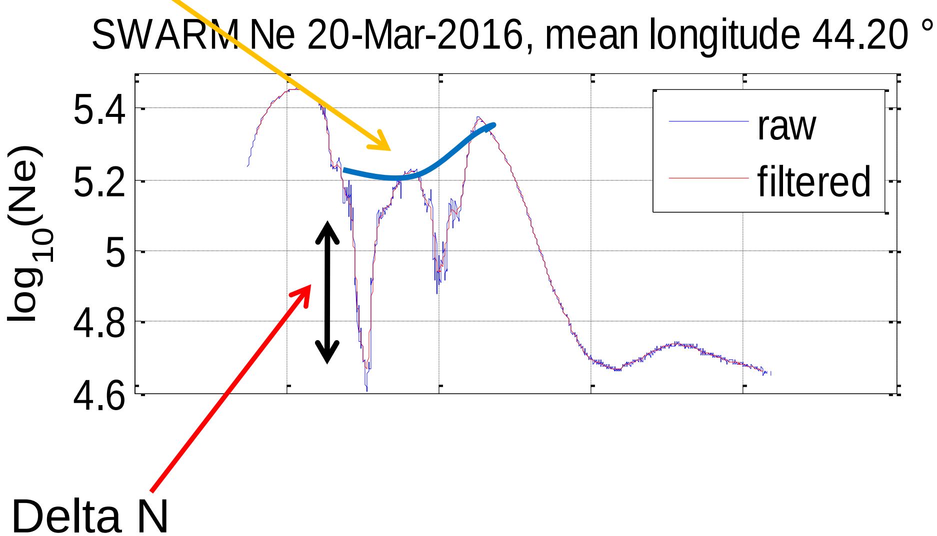

$$RODI = \sqrt{\langle ROD^2 \rangle - \langle ROD \rangle^2}$$

$ROD = d(N_e)/dt$ *is the* rate of change of the detrended in-situ electron density.

RODI was first mentioned by Zhakharenkove et al., 2016 and Compared it to ROTI derived from GPS receiver onboard CHAMP.

Multi-scale structures seen in situ electron density

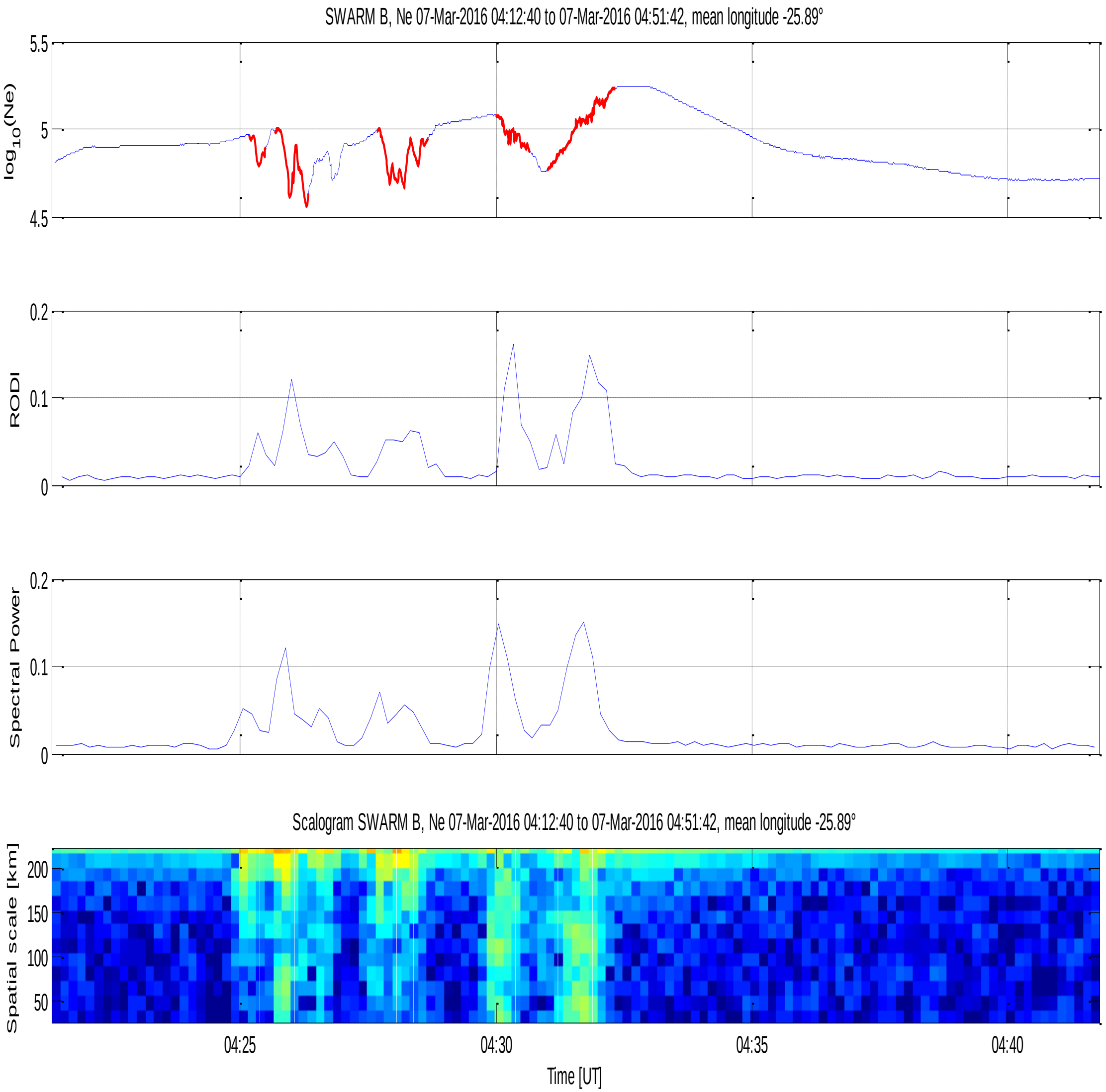

RODI closely follows the Spectral power, which allows us to infer that the RODI is indicative of the high-frequency fluctuations in the frequency band 0.15 Hz to 0.5 Hz.

Periodograms to Scalogram

Period=1/frequency

Scale = period * orbit velocity

Observation of Irregularities from single station:

Diurnal Variation from a lone station:

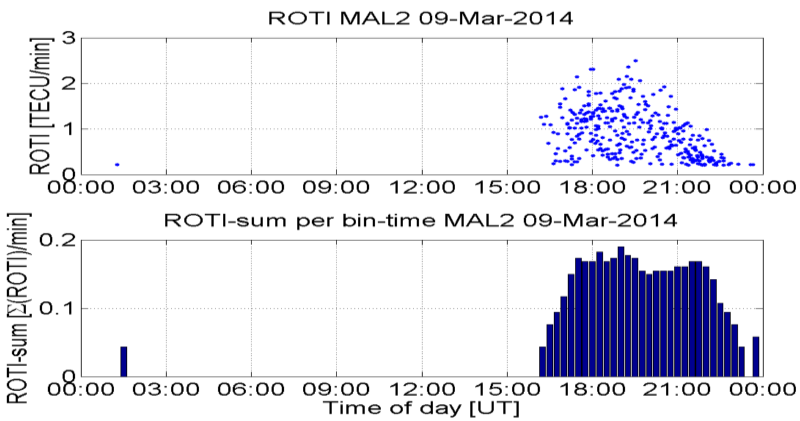

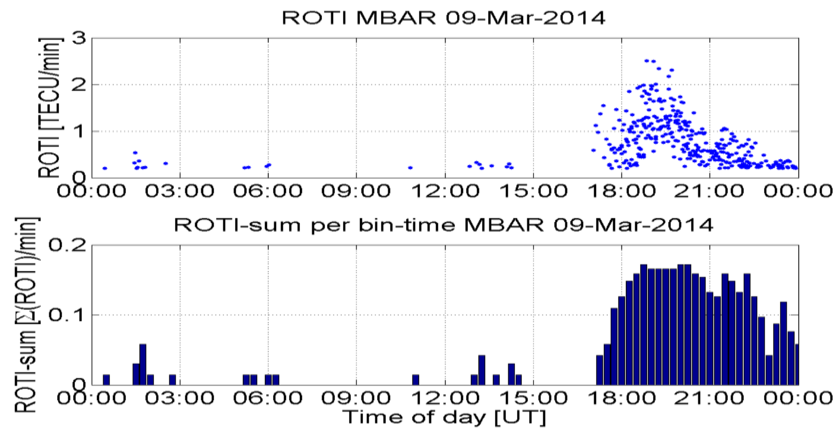

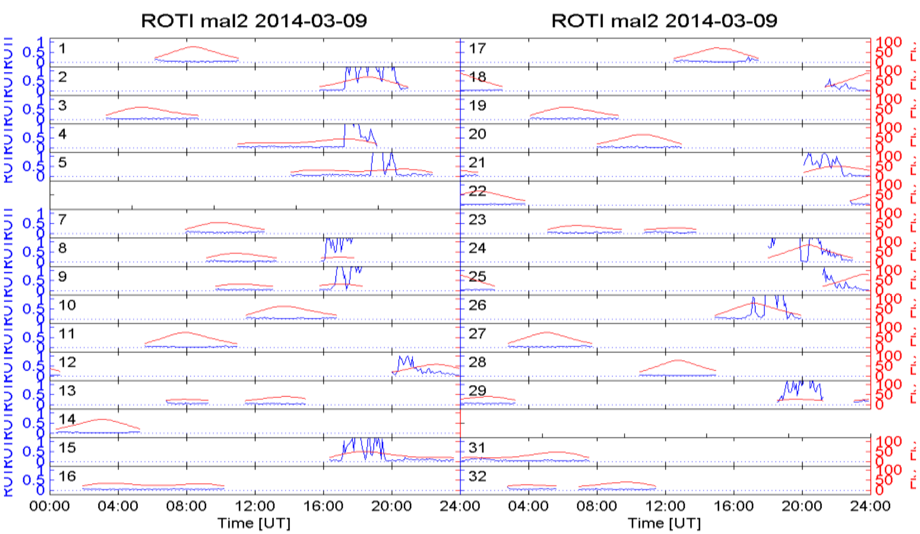

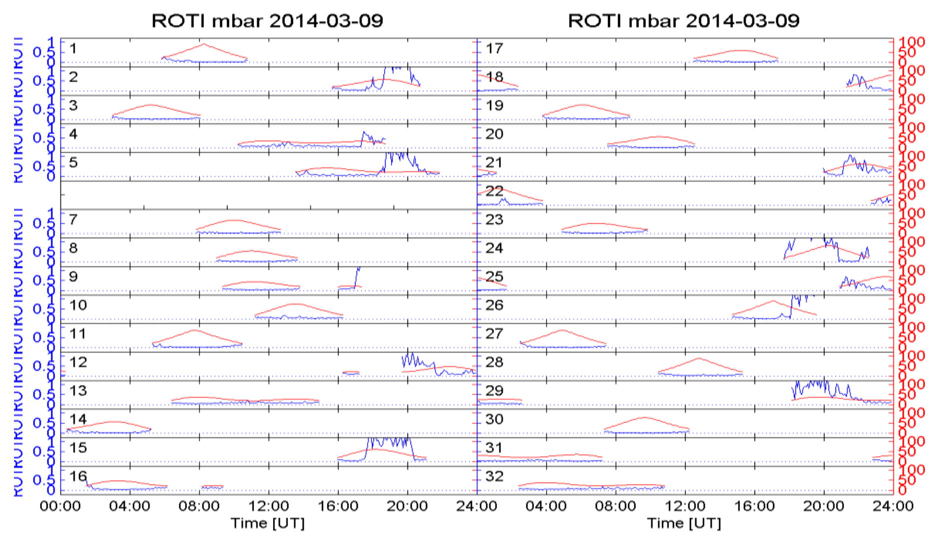

- ROTI fluctuations are significant after 18:00 UT (post sunset hours).
- Spurious spikes that are evident in ROTI measurements must be cleaned out.
- Setting a threshold above which any ROTI measurement is discarded is essential.

Spatial Distribution of irregularities

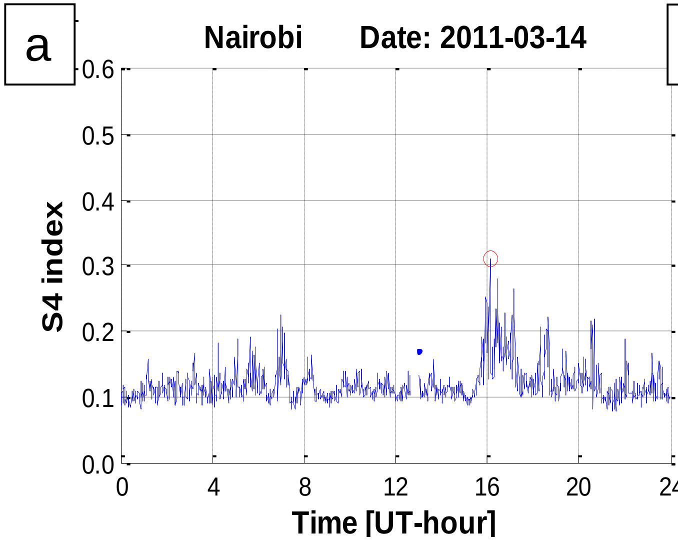

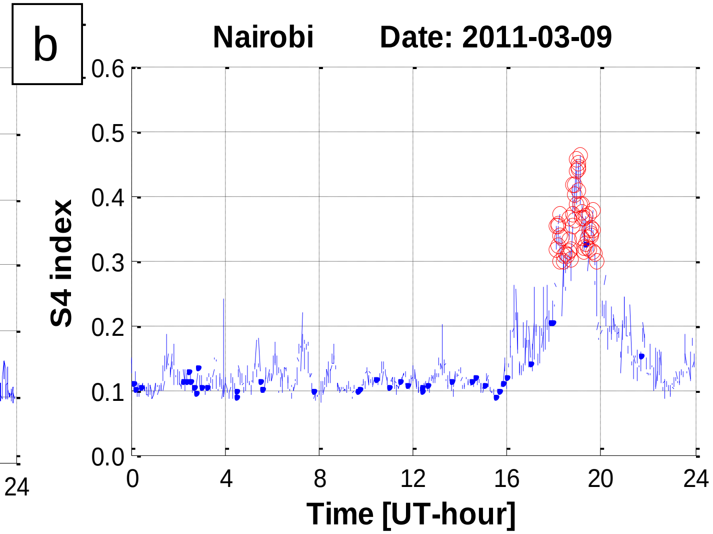

Temporal variation of S4 is already well known to some level

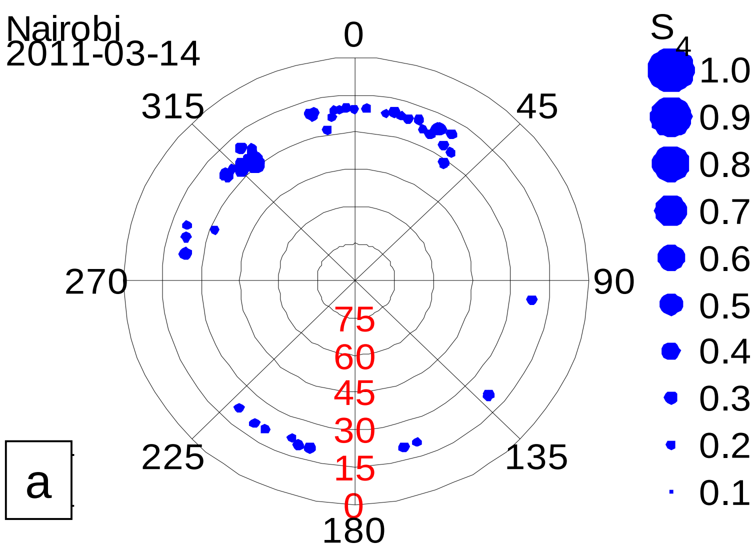

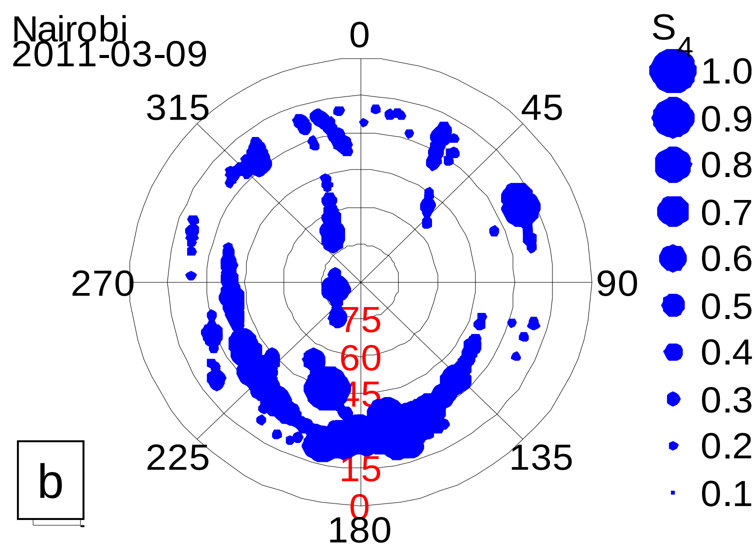

Spatial distribution of irregularities causing scintillation

Spatial distribution of irregularities and the ionization anomaly crests

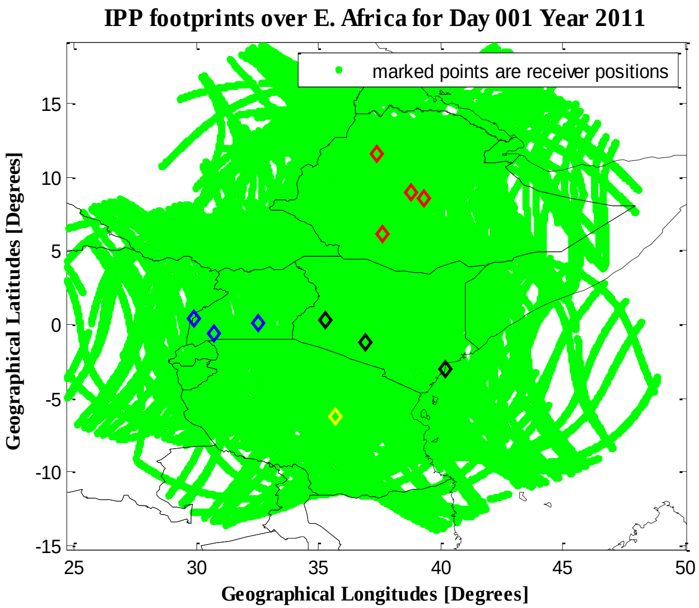

$$TEC(\lambda,\phi)=\sum_{n=0}^{N}\sum_{m=0}^{a}\overline{P_{nm}}[\cos(\phi)]\{a_{nm}\sin(m\lambda)+b_{nm}\cos(m\lambda)\}$$

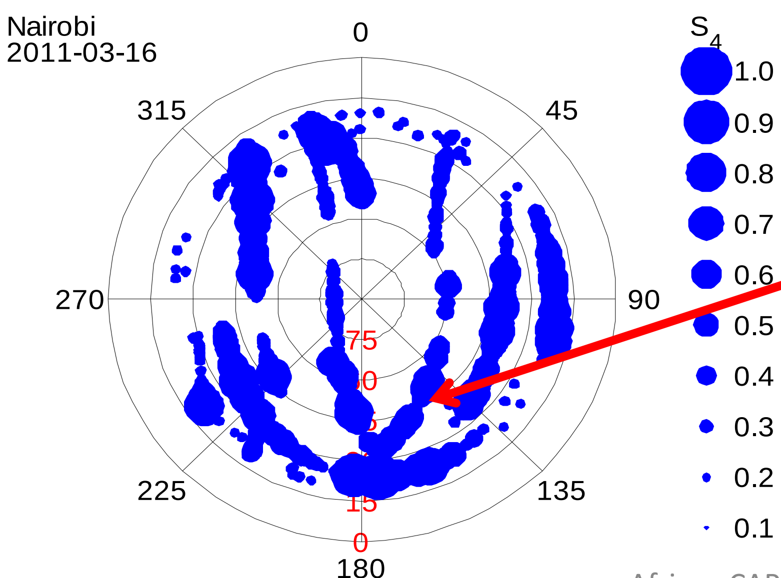

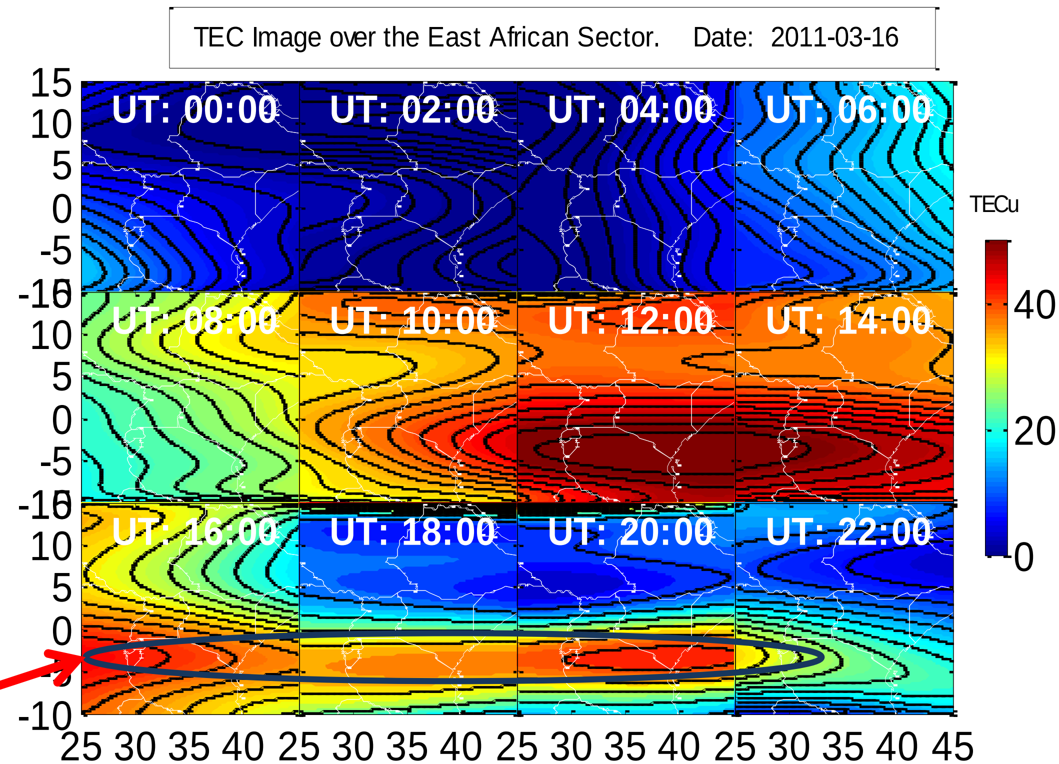

Ionospheric irregularities are within the region with high background electron density – The Equatorial Ionization Anomaly (EIA)

Spatial distribution of irregularities: A climatology from a single station

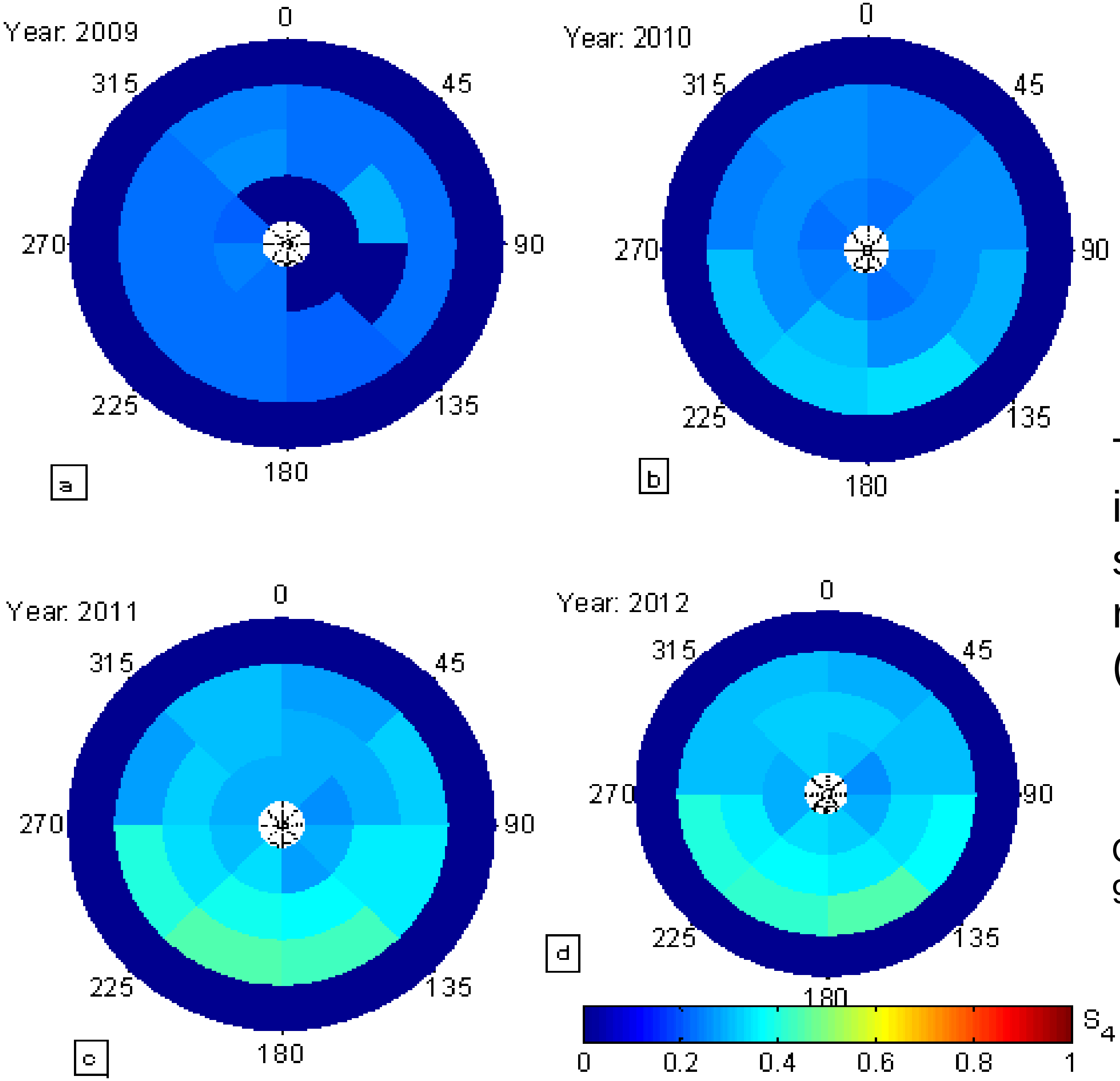

The S4 values are stronger in the Southern parts of the sky as viewed from the receiver location in Nairobi (Kenya)

Olwendo et al., 138-139 (2016), 9-22, JASTP

Diurnal Variation in irregularities across Africa:

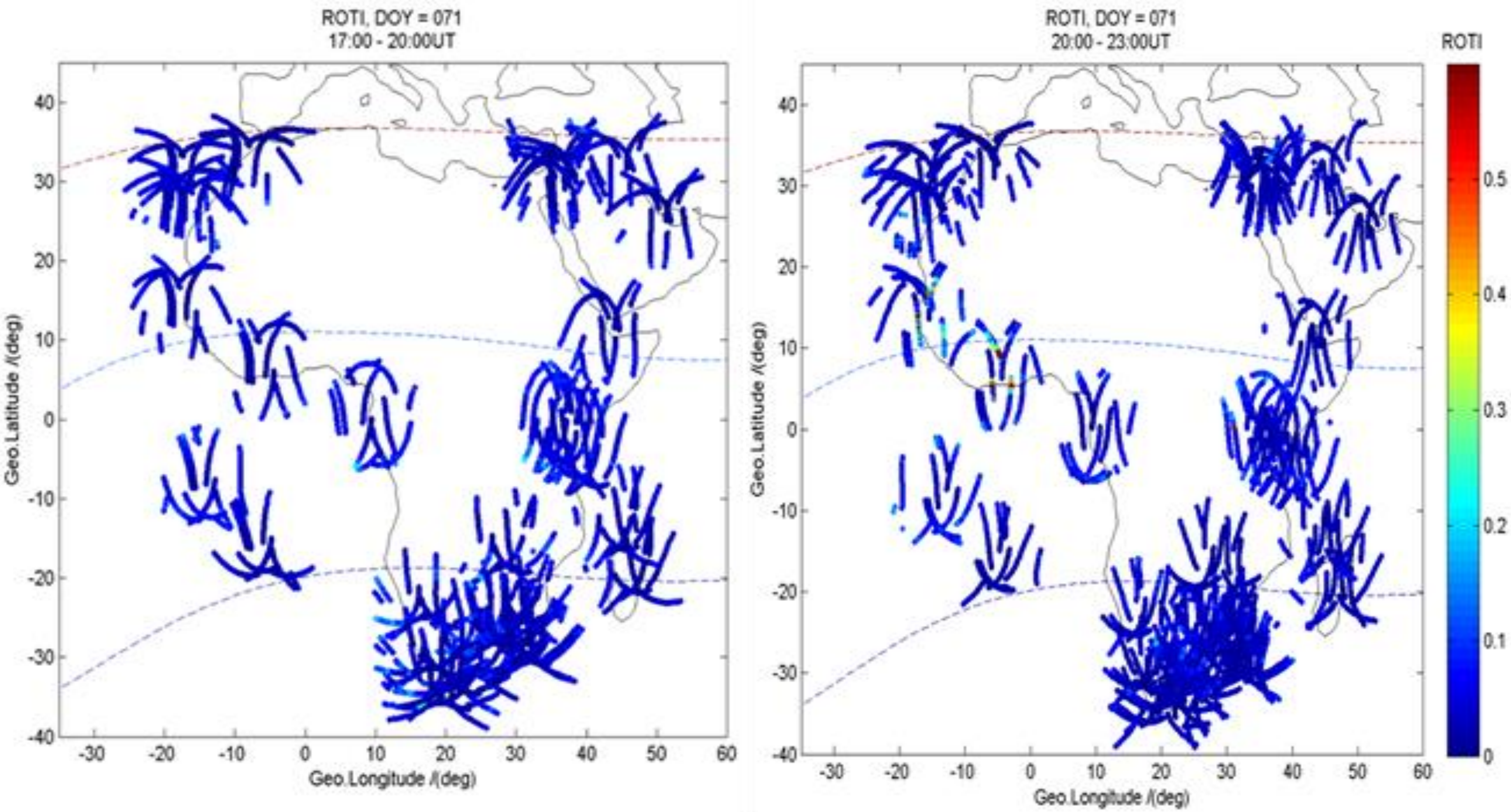

Quiet-time observations of Rate of Total Electron Content Index (ROTI) in the range [0 0.6] for 11 March 2016 (day 71) during the periods 17:00-20:00 UT (left) and 20:00 to 23:00 UT (right). These maps over two 3-hour periods effectively depict the coverage by the available GNSS receivers.

Daily variation of Irregularities: Year of observation-2014

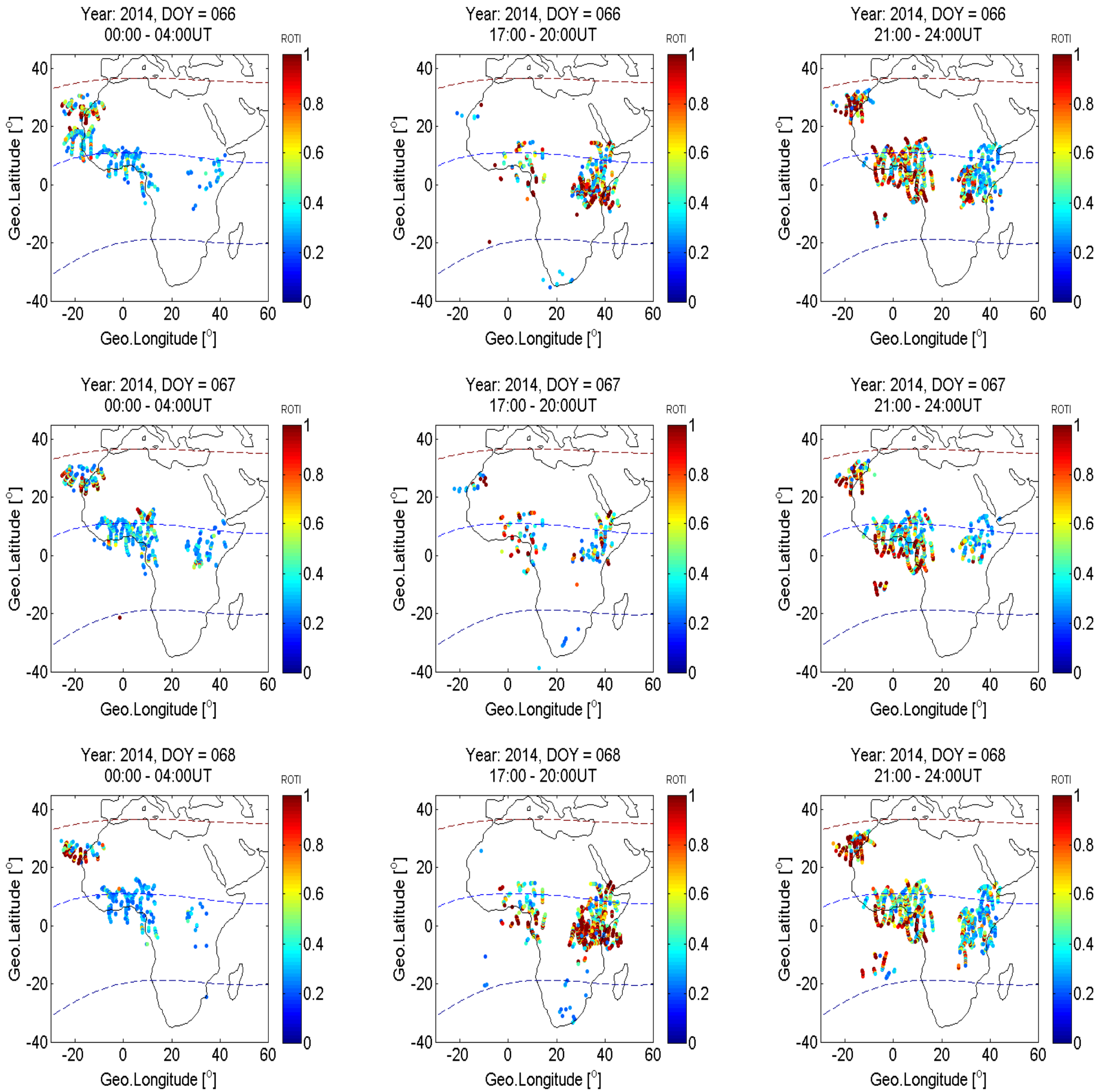

Temporal and spatial distribution of ionospheric irregularities (ROTI>0.2) across the African region during 7 to 9 March 2014 (days 66 to 68).

Daily variation of Irregularities: Year of observation-2020

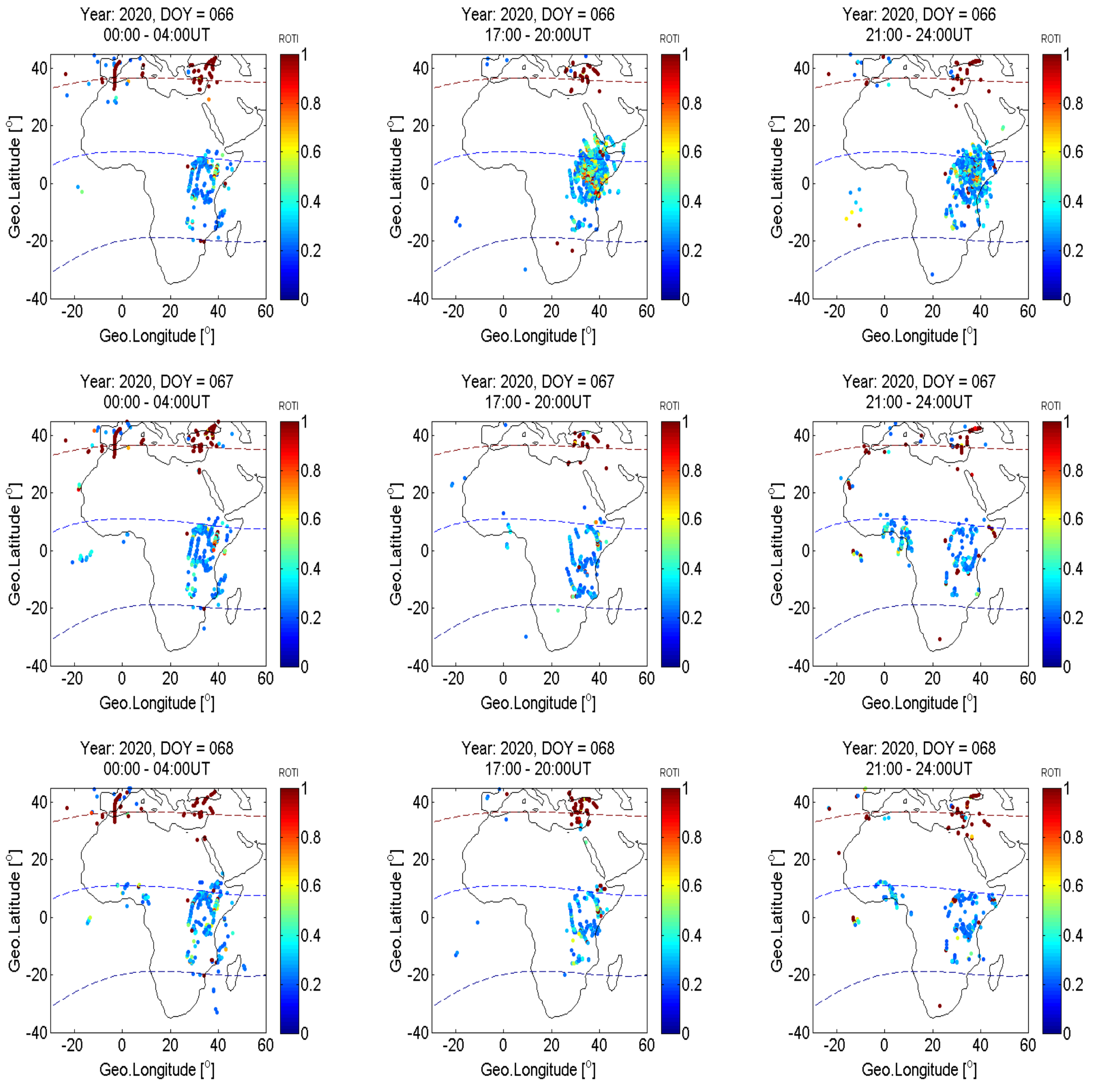

Temporal and spatial distribution of ionospheric irregularities (ROTI>0.2) across the African region during 6 to 8 March 2020 (days 66 to 68).

Coincidental space-based and ground-based observations: Across Africa

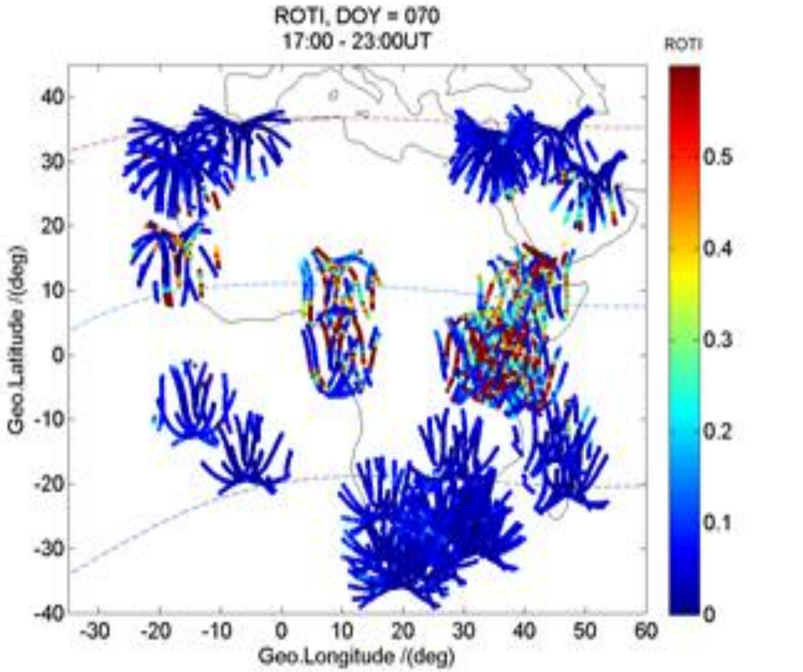

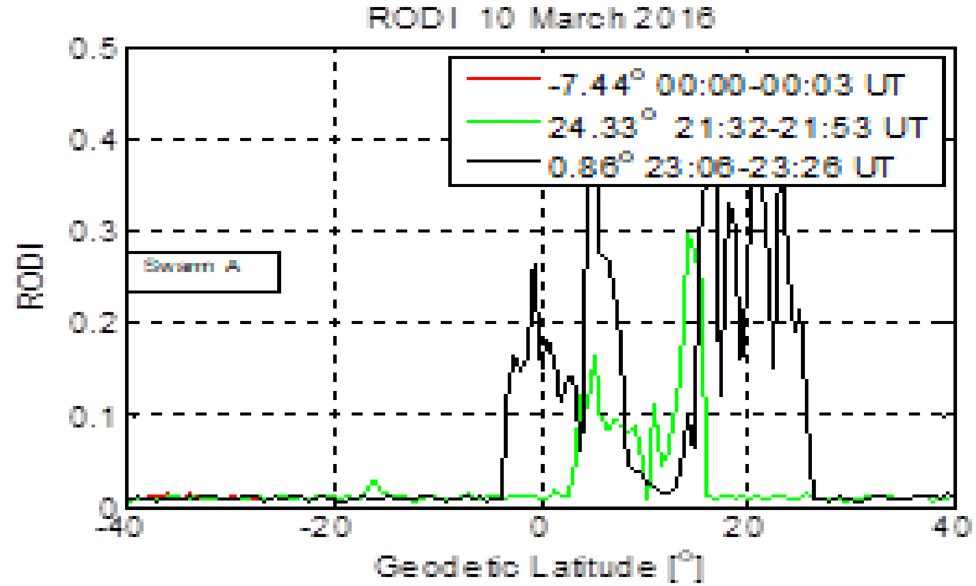

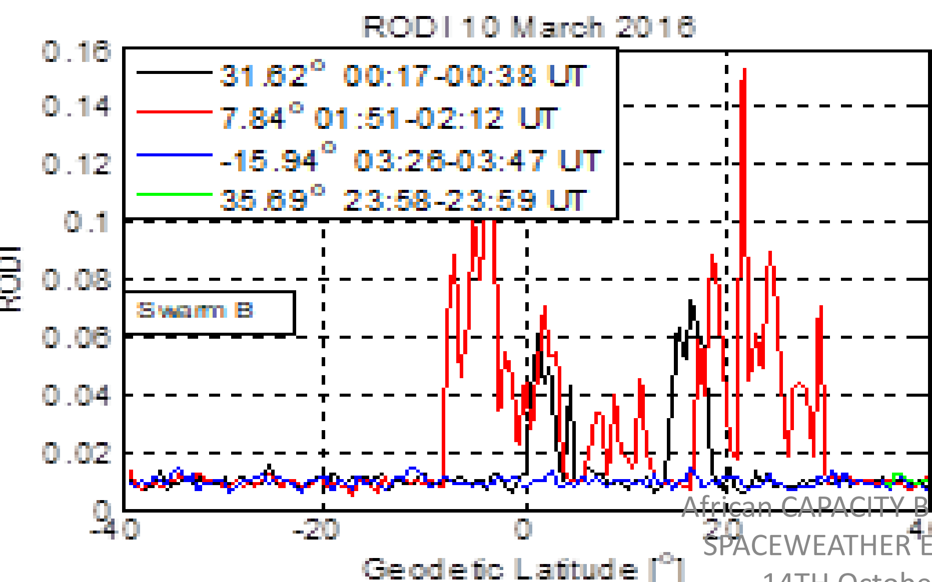

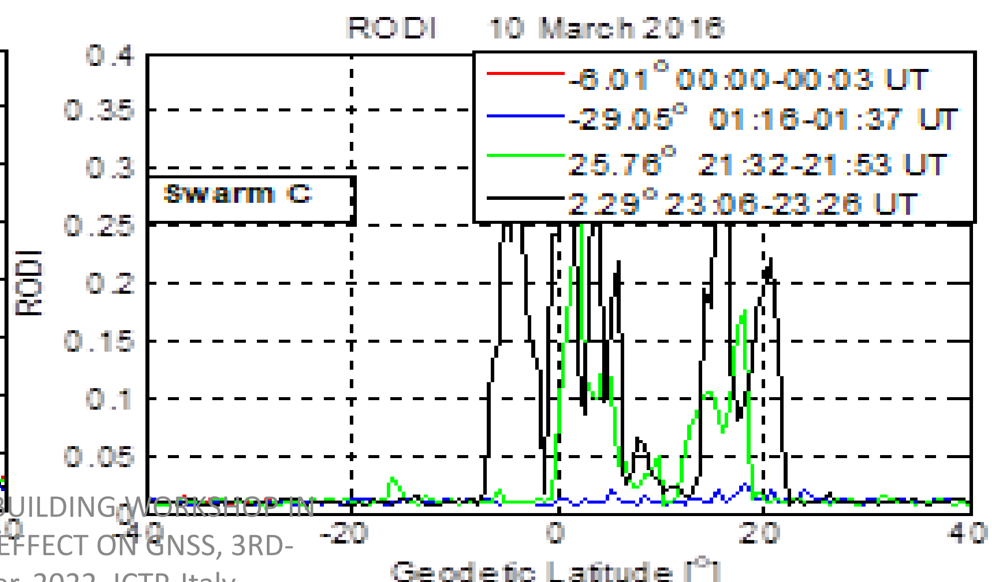

Using LEO to fill the gaps in data coverage across Africa: Swarm, CHAMP etc

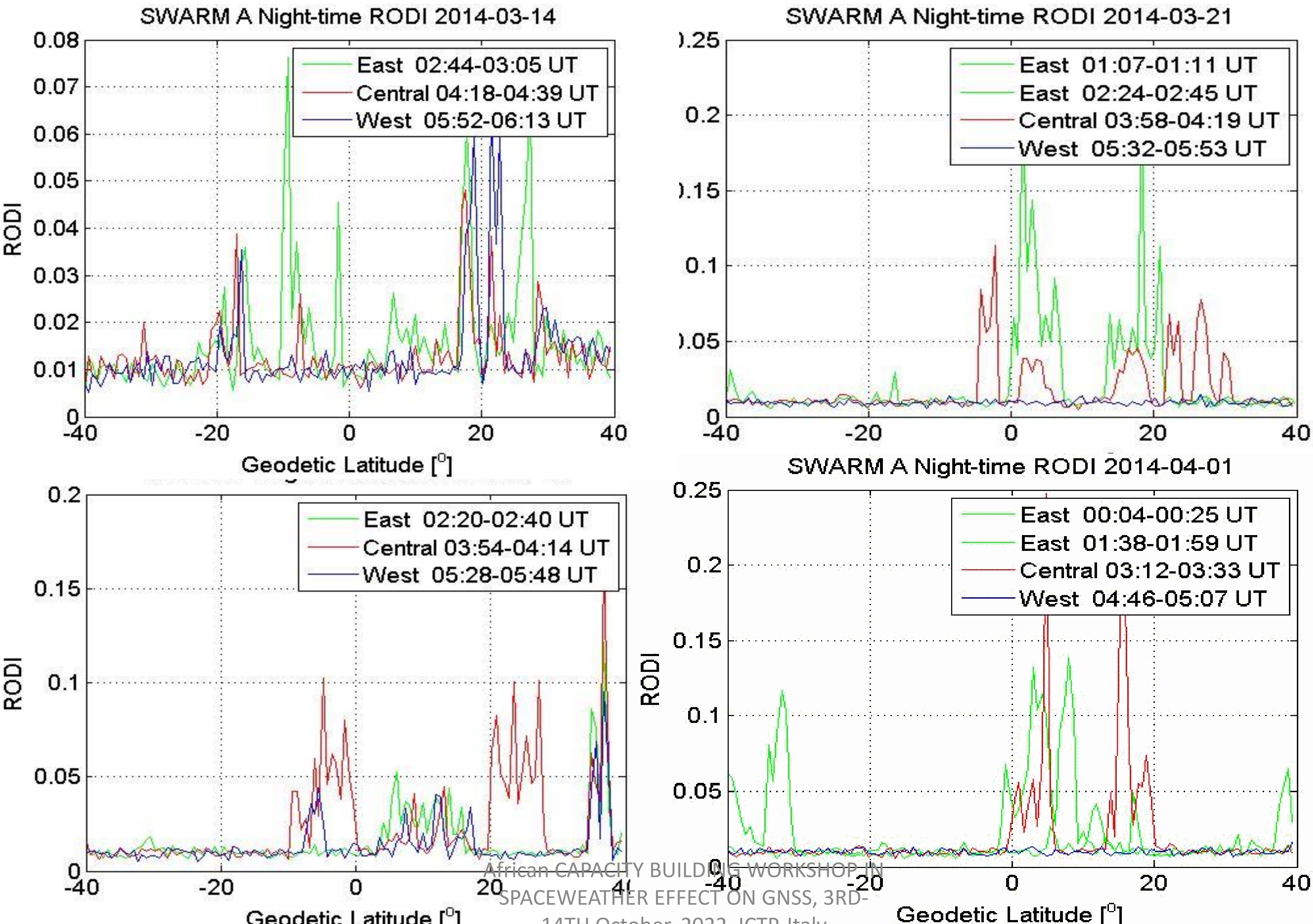

Annual variability over Africa in 2014

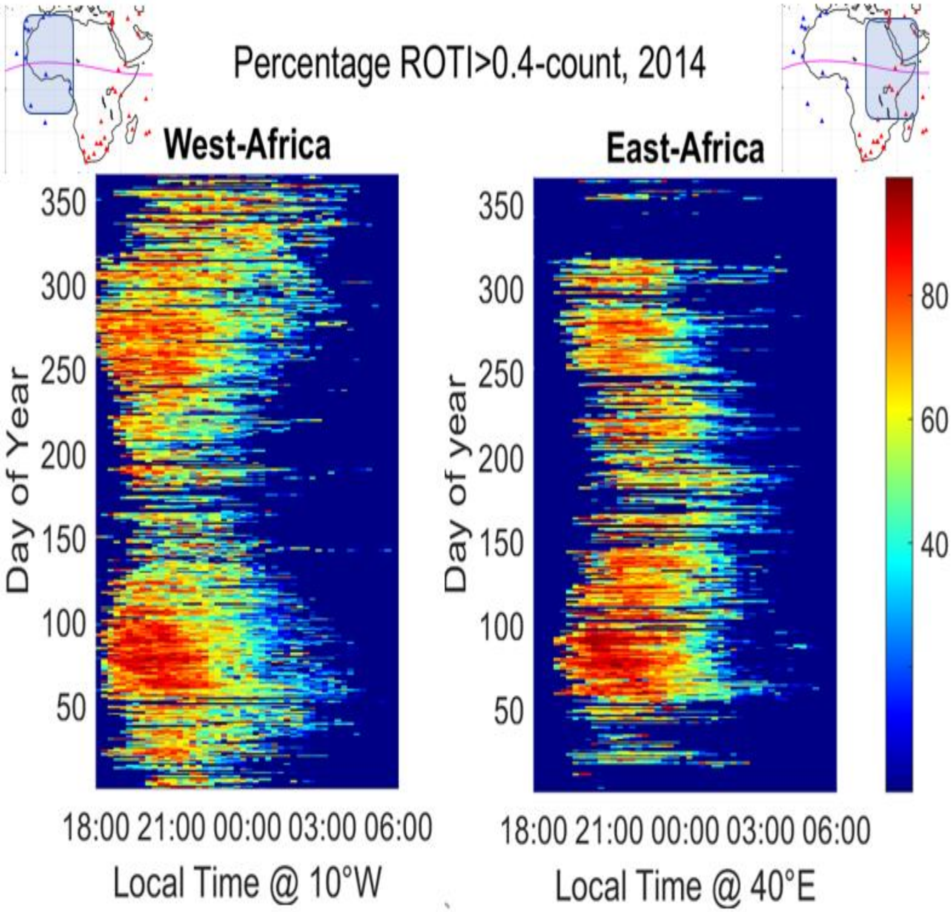

Ionospheric irregularity activity distribution across the African region based on the percentage of ROTI counts above 0.4 for the year 2014 for stations located on the western side (on the left) and stations located to the eastern side (on the right).

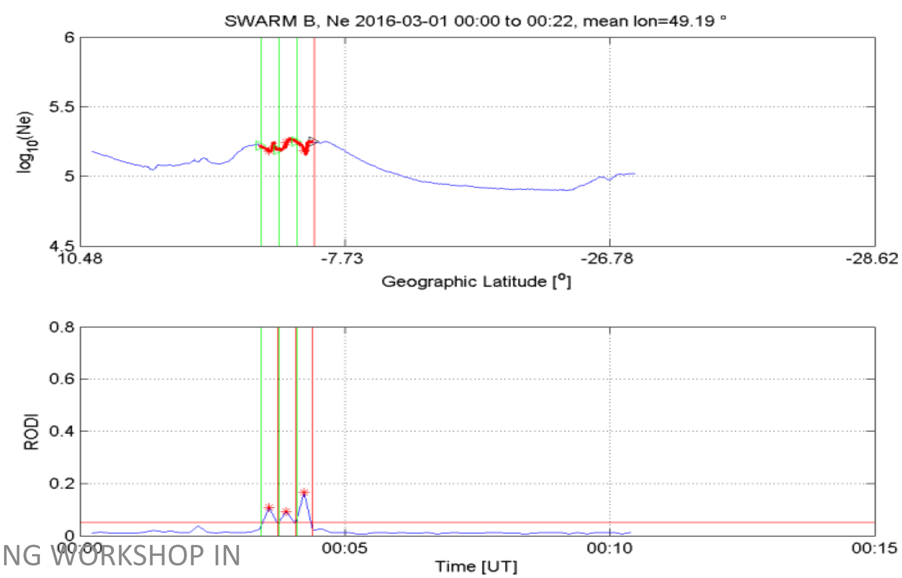

From the Swarm data shown, there seems to be a much intense irregularity activity on the West side of Africa than the East.

On morphology of irregularities: Year of Observation 2019
What shape do irregularities take? The inverted C-shell structure!!

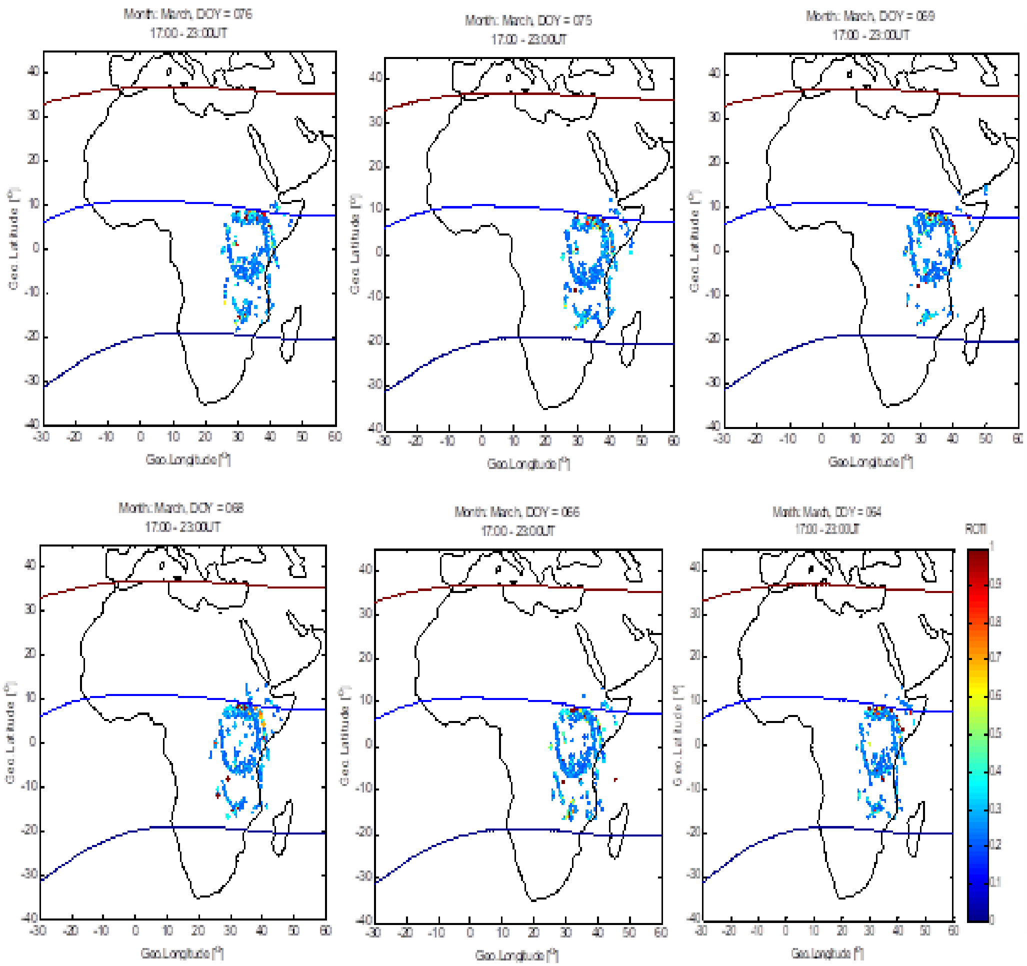

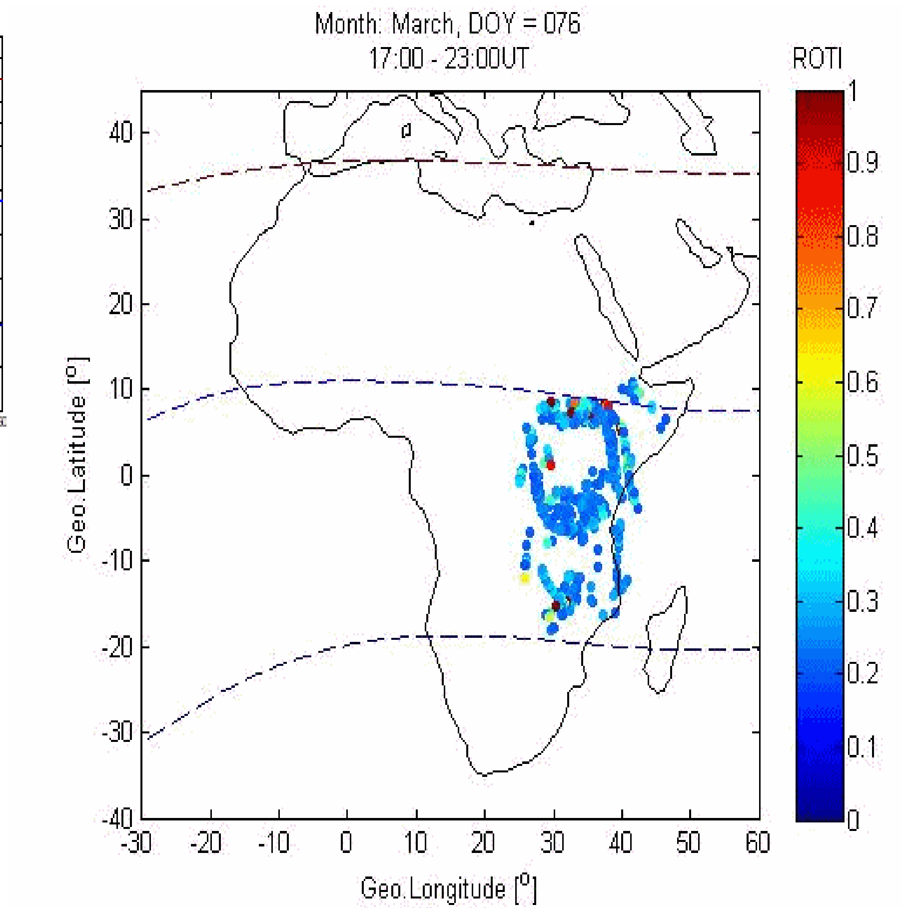

Plasma bubbles: vertically elongated wedges of depleted plasma that drift upward then eastward/dip equator and downwards towards the southern hemisphere followed by an inward inverted C structure towards the west and toward the dip equator.

Other forms of irregularities associated with post-sunset TEC perturbation: based on dTEC measurements

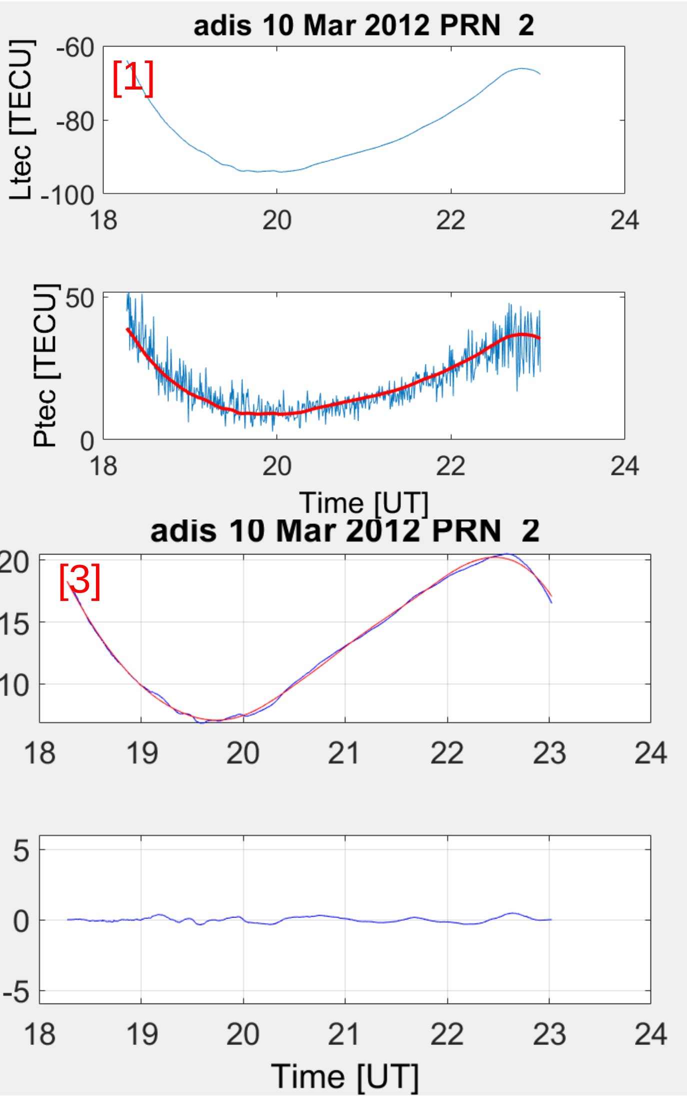

Steps in the derivation of the dTEC

Panel [1]: Level shifting of slant Ltec using mean of slant Ptec over each arc

Panel [2] Plot of level shifted sTEC and pTEC with elevation

Panel [3] Plot of each arc of vTEC, vTEC smoothed and dTEC (in this case there was only one arc)

Panel [4] Plot of vTEC, smoothed vTEC and dTEC for the selected PRN

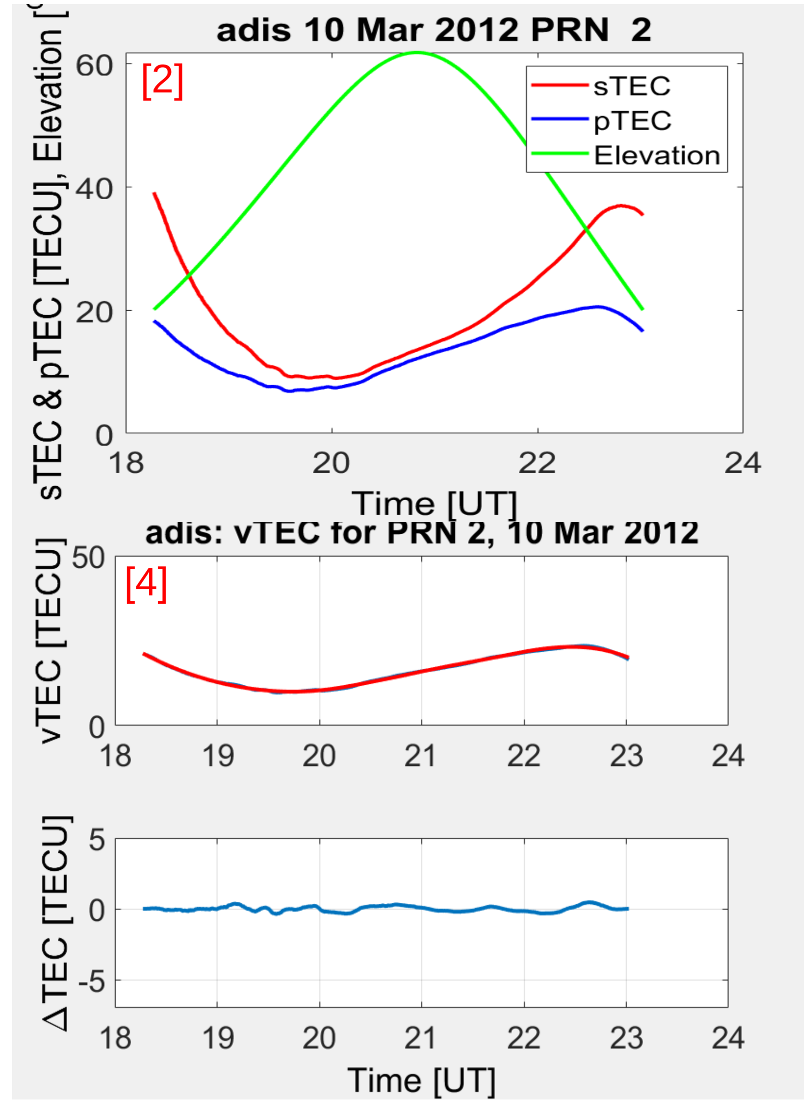

Comparison of different techniquesfor dTEC computation

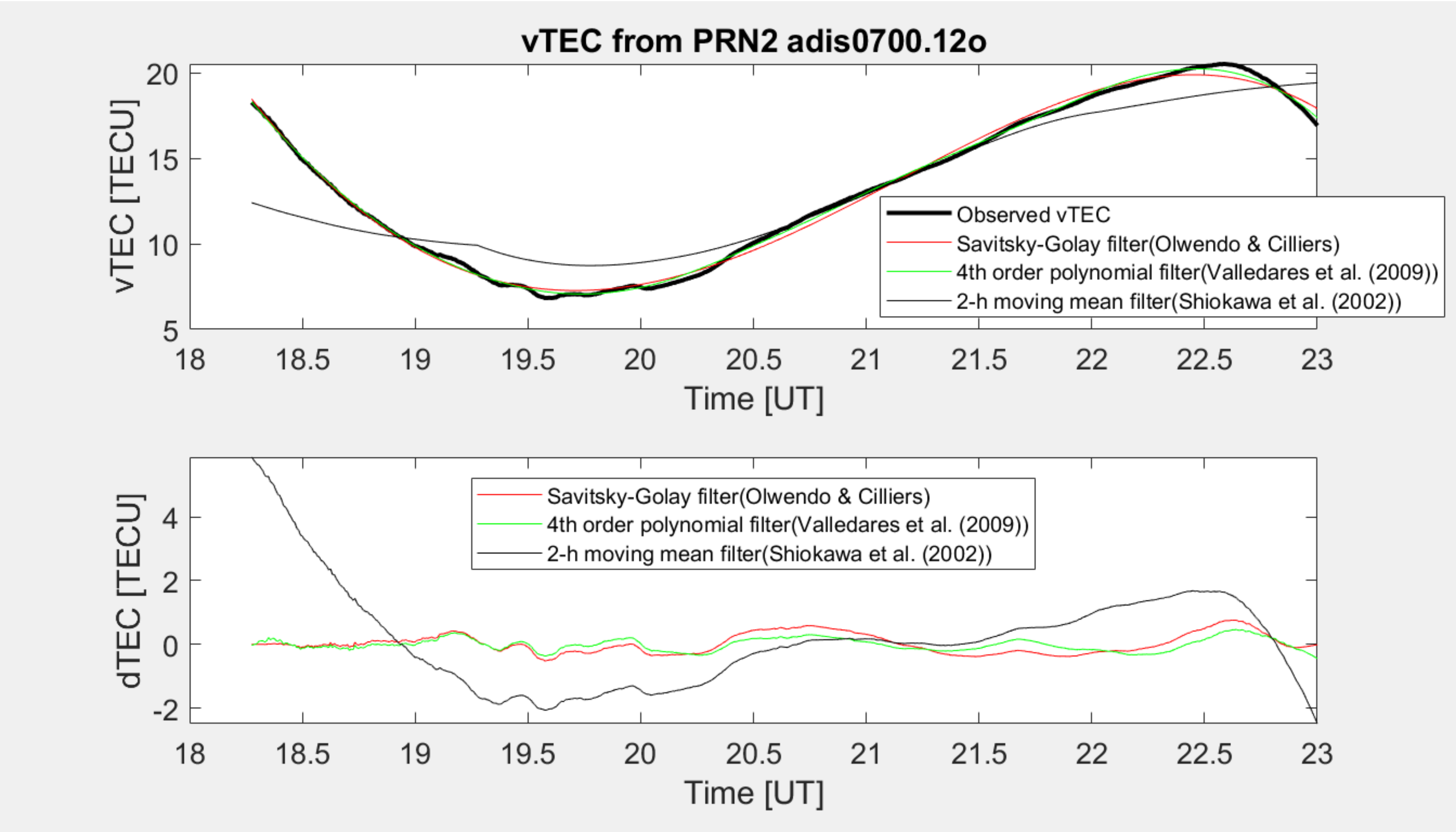

Spectra of dTEC for different smoothing filters

Data : adis 0700.12o, PRN 2

Savitsky-Golay (Olwendo & Cilliers)

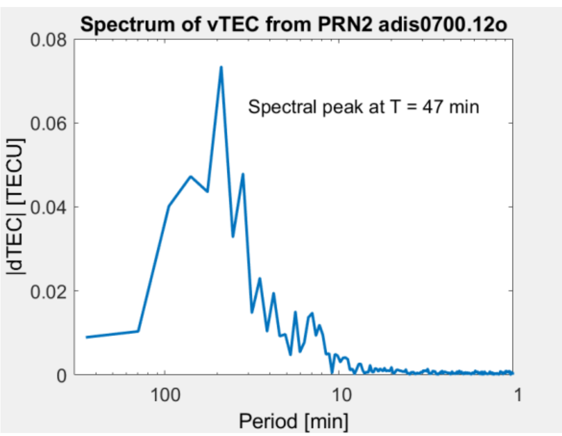

4th order polynomial filter (Valledares et al. (2009))

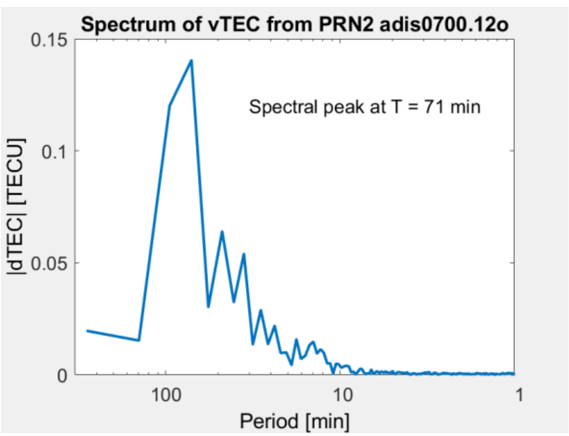

2 hour moving mean filter (Shiokawa et al. (2002))

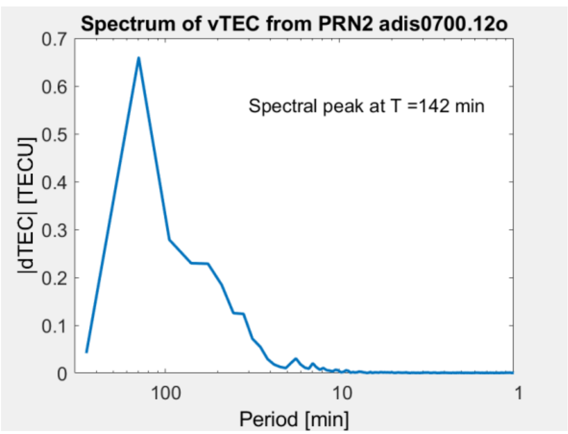

Note that the spectra of dTEC depends very strongly on the filtering technique used for smoothing the vTEC arcs before deriving dTEC. The dominanf periods (period of spectral peak) of the FFT of dTEC will strongly depend on the filtering technique. Our work uses the Savitsky-Golay filter.

TEC perturbation: spectra associated with dTEC measurements

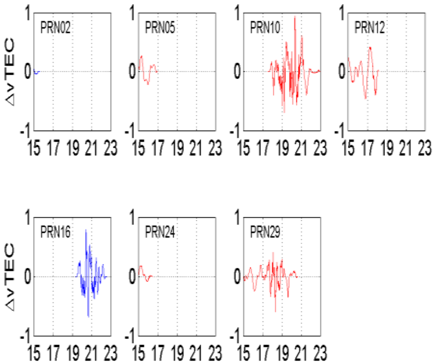

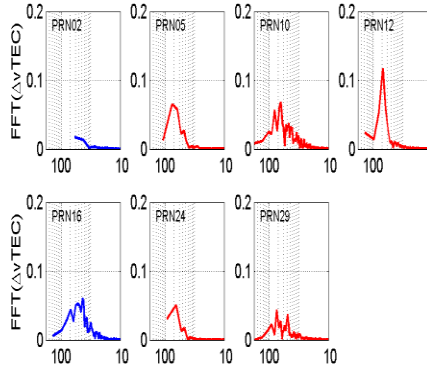

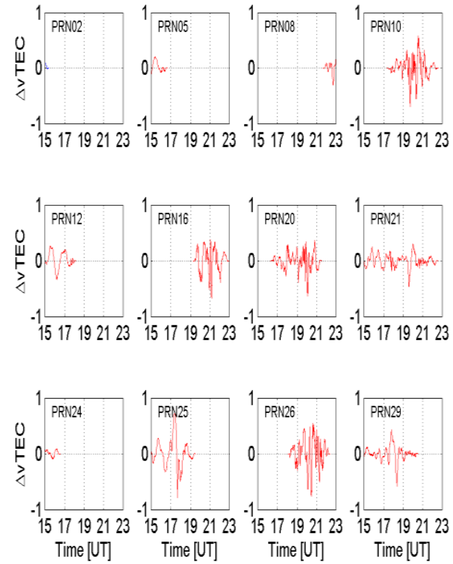

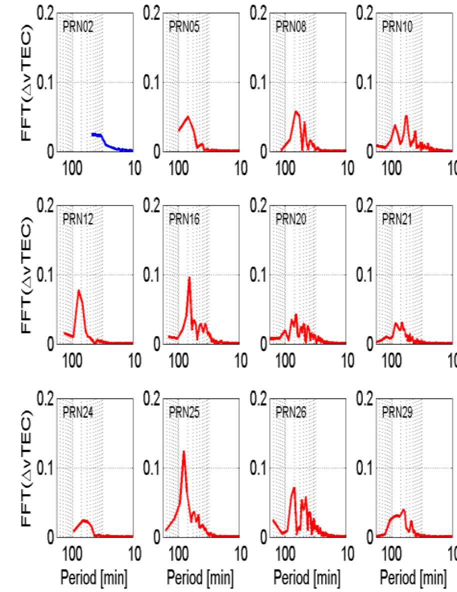

Blue = rejected dTEC measurements

Red = accepted dTEC measurements

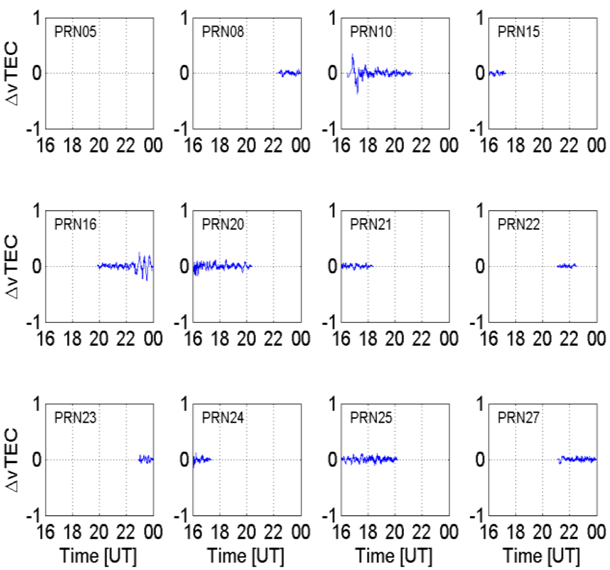

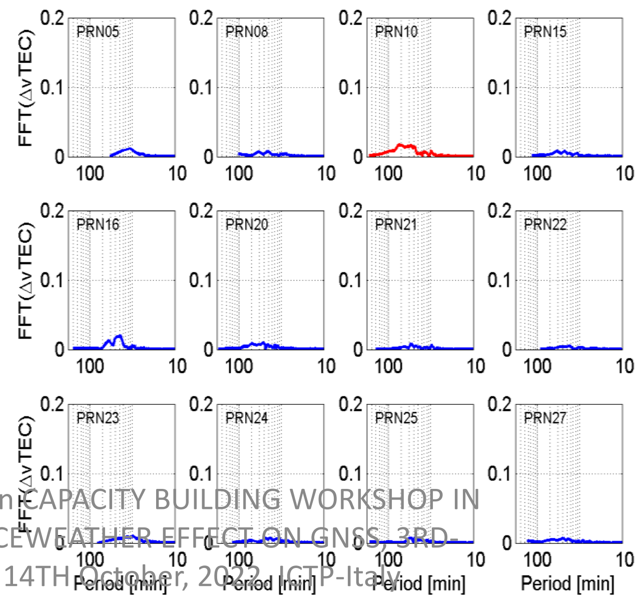

dTEC measurements are selected by their spectral properties to reduce noise:

1. Spectral amplitude must be above the noise level
2. Spectral peak must lie within typical range of frequencies

Propagation characteristics of the dtec

dTEC integrated over longitude range 15º-45º E
(with spectral filtering, fast algorithm)

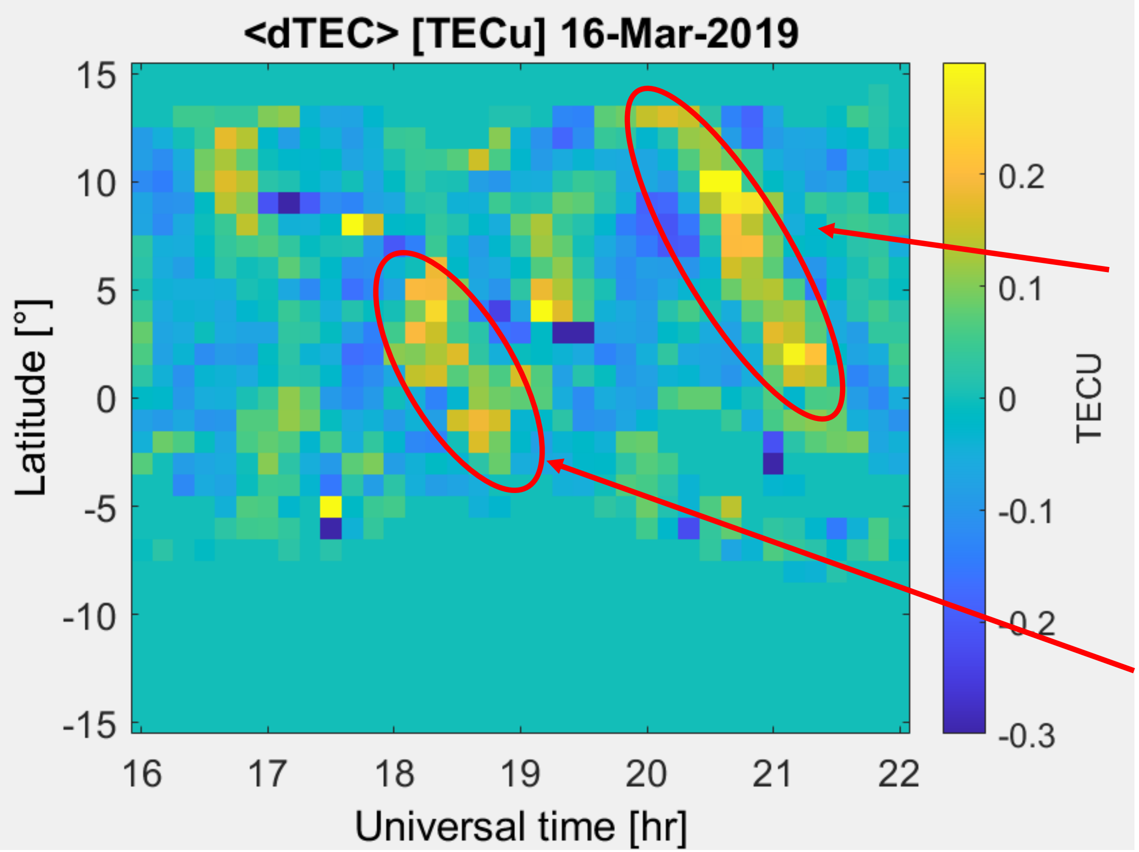

There seems to be a Southward moving wave of which the crest near 10ºN is well developed by 20:30 UT. This crest moves Southward to 0º by 21:00

A second crest starts forming at 18:00 at 5ºN and propagates Southward to 2ºS by 18:30 UT

dTEC integrated over longitude range 15º-45º E (with spectral filtering, fast algorithm)

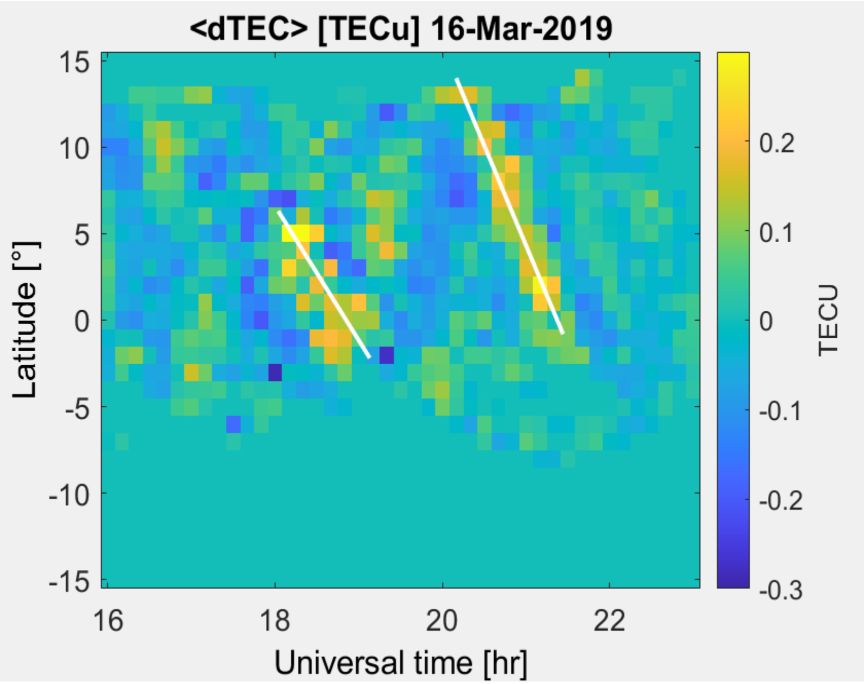

Manual selection of slopes of TID crests

16 Mar 2019 dTEC_file='Af_dtEC_19075.mat';
The average velocity of crest 1 is 357.15 m/s Southward
The average velocity of crest 2 is 239.49 m/s Southward
TID period at time 19.7 UT = 2.7 hours
TID wavelength at latitude 3.7° = 2878 km

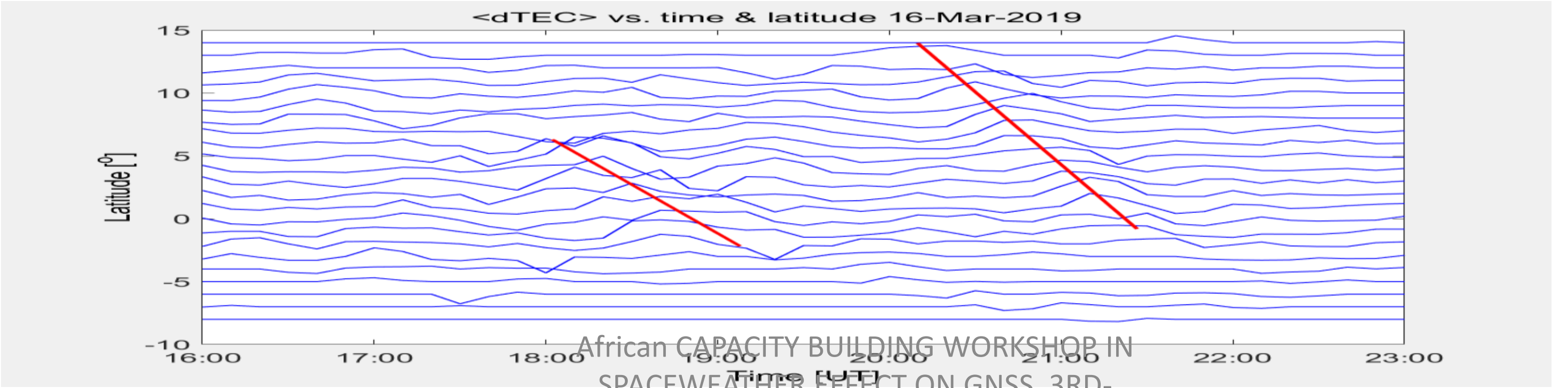

Does this TEC perturbation energy impact irregularity dynamics ?

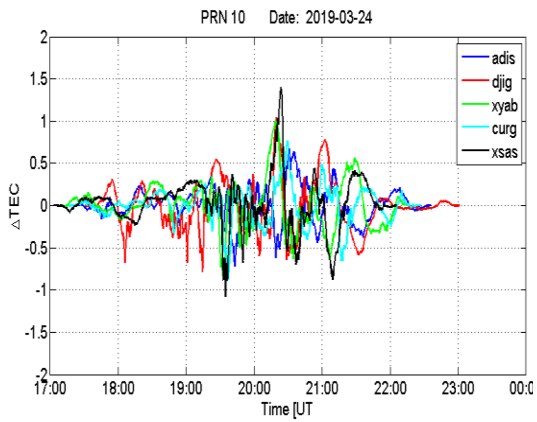

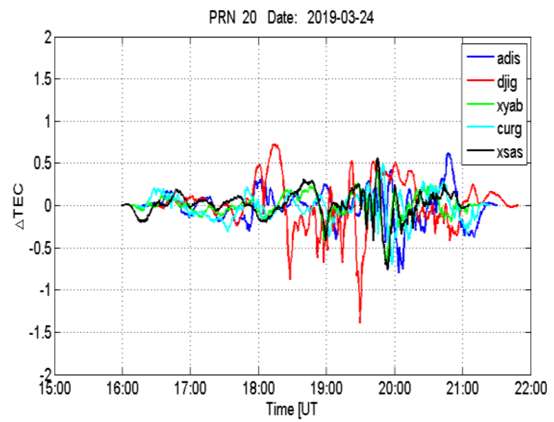

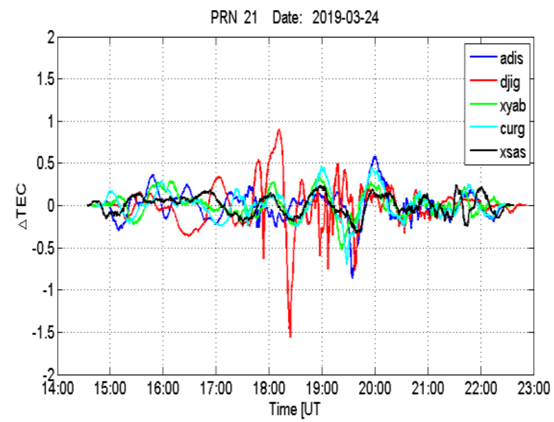

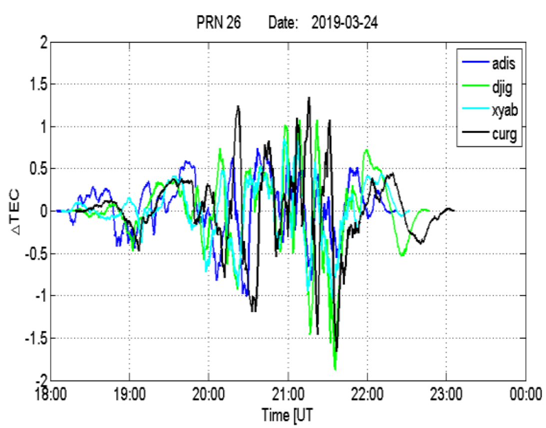

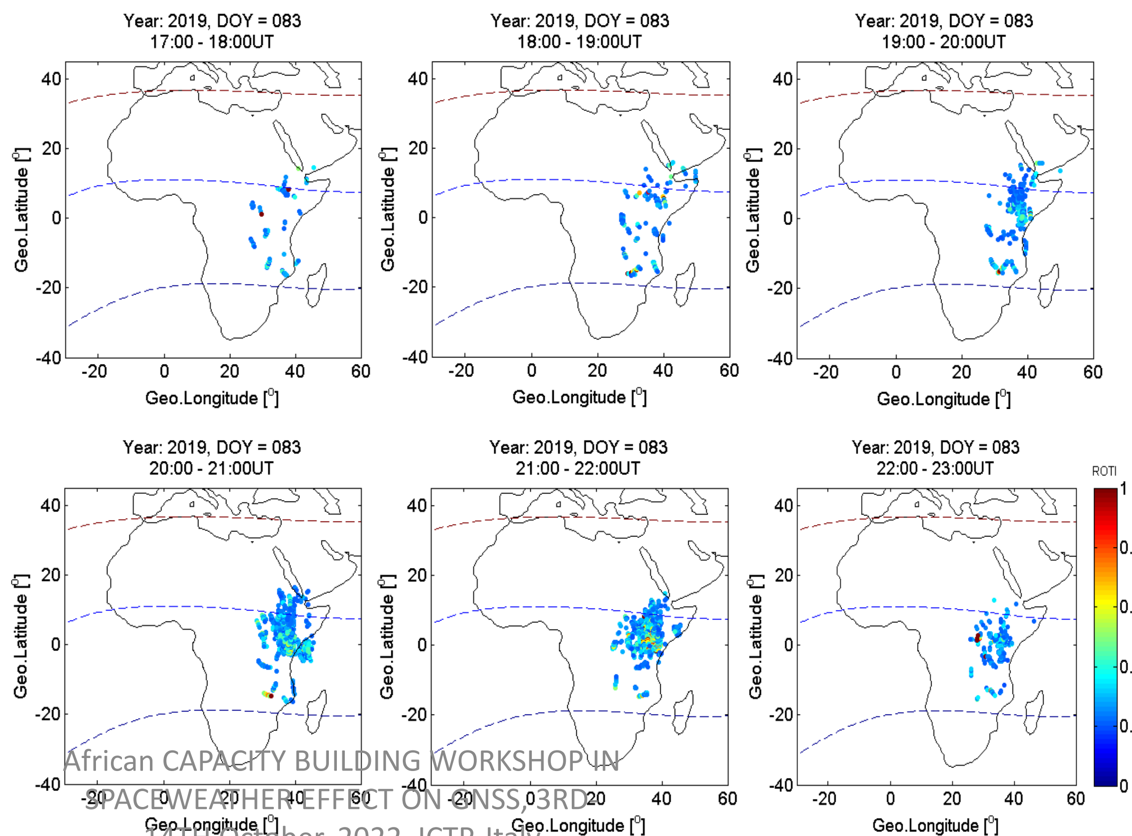

Summary on irregularities at low latitudes

The general features of the irregularities are:

1. Plasma irregularities generally occur after ~20:00 LT and continue for about an hour to several hours and sometimes until sunrise.

2. Post-sunset irregularities are frequent, intense and last longer centered around the magnetic equator at equinoxes especially at high solar activity.

3. The irregularities usually start appearing in the bottom-side ionosphere when it raises above a threshold height that varies with various geophysical conditions.

4. The irregularities quickly rise to high altitudes well beyond the ionospheric peak, sometimes rising beyond 2000 km at the equator.

Summary on irregularities at low latitudes (continued)

5. As the irregularities rise in altitude, they move poleward aligned along the geomagnetic field lines, reaching up to ±30° magnetic latitudes in extreme cases.

6. The irregularities usually drift eastward with velocity in the range of 100 to 200 m/s.

7. Geomagnetic activity intensifies the irregularities in some cases and inhibits them in other cases.

References

•Hargreaves, J. K., Auroral absorption of HF radio waves in the ionosphere: a review of results from the first decade of riometry(1969), Proc. IEEE, 57, 1348-1373, 1969.

•Olsen, N., C. Stolle, R. Floberghagen, G. Hulot, A. Kuvshinov, (2016), Special issue 'Swarm science results after 2 years in Space', Earth, Planets and Space, 68:172, doi:10.1186/s40623-016-0546-6.

•Olwendo, O. J., et al., (2012), Using GPS-SCINDA observations to study the correlation between scintillation, total electron content enhancement and depletion over the Kenya region. Adv. Space Res., 49, 1363-1372, doi:10.1016/j.asr.2012.02.006.

•Olwendo, O. J., et al., (2016), Low latitude ionospheric scintillation and zonal plasma irregularity drifts climatology around the equatorial anomaly crest over Kenya. J. Atmos. Sol.- Terr. Phys., 138-139, 9-22.

•Park, J., et al., (2005), Global distribution of equatorial plasma bubbles in the pre-midnight sector during solar maximum as observed by KOMPSAT-1 and Defense meteorological Satellite Program F15, J. Geophys. Res., 110, A07308.

•Paznukhov, V. V., et al., (2012) Equatorial plasma bubbles and L-band scintillations in Africa during solar minimum. Ann. Geophys., 30, 675-682.

•Pi., X., Mannucci, A.J., Lindqwister, U.J., and C.M. Ho., *Geophys. Res. Lett., 24, 2283, 1997.*

•Yizengaw, E., et al., (2013), Post-midnight bubbles and scintillation in the quiet-time June solstice. Geophys. Res. Lett. 40, 5592-5597.

•Zakharenkova, I., and E. Astafyeva (2015), Topside ionospheric irregularities as seen from multisatellite observations. J. Geophys. Res. Space Physics 120, 807-824.